

Comparison of
Orbital Proton Fluences
For Typical Mission Orbits

Jess Johnson

Senior Instrumentation Scientist
Steward Observatory, University of Arizona
September 28, 2023

Abstract

This paper compares proton fluxes for four typical mission orbits: the MEO orbit; the Molniya HEO orbit; the TESS P/2 HEO orbit, and the Spitzer Earth Trailing orbit (ETO); for more detail on individual orbits, see the Orbital Comparison memo. The proton fluxes are the result of SPENVIS modeling, with the exception of the ETO, which is cited from Spitzer data. Illustrations of the orbital paths and their proximity to the Van Allen Radiation Belts are also presented.

Author's note: This memo has gone through substantial revision since its original posting. I have made a few tweaks to the P/2 HEO trajectory input in the SPENVIS orbit model, which corrected a geometry error in the original orbit. This has resulted in the P/2's fluence values to change considerably. I caught the mistake by realizing that the P/2 should not be generating significant trapped particle fluence as it lies completely outside the Van Allen belts. The values in this revision reflect this correction.

Contents

1	Introduction	3
2	A few Notes	3
2.1	Reading the Simulation Output	3
2.2	Integral vs. Differential Spectra	3
2.3	Effects of Trapped Particle Radiation on Spacecraft Components	3
3	Orbits	4
3.1	MEO-Type Orbits	5
3.1.1	The Medium Earth Orbit	5
3.1.2	The Equatorial Medium Earth Orbit	5
3.2	Molniya Orbit	6
3.3	P/2-HEO Orbit (TESS)	8
3.4	Earth-Trailing Orbit	8
3.4.1	Description	8
4	Orbit Radiation	9
4.1	A few Notes	9
4.1.1	Note on ETO Radiation Data	9
4.1.2	Notes on Simulations	10
4.2	MEO Orbit Simulations	11
4.2.1	Trapped Proton Fluxes and Fluences	11
4.2.2	Solar Particle Fluences	11
4.3	Molniya Orbit Simulations	11
4.3.1	Trapped Proton Fluxes and Fluences	11
4.3.2	Solar Particle Fluences	11
4.4	P/2 HEO TESS Orbit Simulations	12
4.4.1	Trapped Proton Fluxes and Fluences	12
4.4.2	Solar Particle Fluences	12
4.5	Earth Trailing Orbit Data	12
5	Radiation Comparisons	15
5.1	Trapped Particle Fluence Comparison	15
5.2	Solar Proton Fluence Comparison	16
6	Conclusions	16
6.1	Trapped Particle Exposure	16
6.2	Solar Proton Exposure	18
6.3	Summary	18
Appendices		19
A	Table of Solar Proton Events	19

1 Introduction

This report shows proton Fluxes and fluences for several different orbits. In all but one case, these are the products of SPENVIS modeling; in the other, they are reproduced from other's work. and are credited as such. SPENVIS is designed to primarily address geocentric orbits; one of the orbits under consideration is a heliocentric orbit.

Although the scope of this paper is limited to high energy proton radiation, a few of the illustrations show the intersection of orbits with the Van Allen Belt electron regions; these are included without further data because the orbit's exposure to these regions warrant concern, and are obvious companion images to the proton region images. High energy electron fluxes and fluences will be addressed in an upcoming report.

Two sets of data for each orbit, excepting the heliocentric orbit, are presented. The first provides fluxes for trapped energetic protons, as well as proton fluences for a mission lifetime of one year. These were run with the standard NASA AP8 model set to simulate conditions of solar maxima. The second provide solar particle fluences under worst case scenarios. The sum of the two is a good representation of what should be the worst case situations for proton bombardment.

Finally, these fluxes and fluences do not take into account any form of shielding that the Pearl mission may implement. The point of this report is to show the radiation environment of individual orbits, so that exposure levels on different orbits can be compared.

2 A few Notes

2.1 Reading the Simulation Output

The SPENVIS flux and fluence tables are read as follows. Column one shows spectral energy bins. Column two shows the total mission *flux*; i.e., the average, over the mission duration, of protons in this energy bin per centimeter squared per second. The third column shows the total mission *fluence*; that is, the flux in this energy bin, integrated over the mission duration. Because these simulations were performed on the science trajectory only, there is only one mission segment, so the contents of columns four and five duplicate the contents of columns two and three.

2.2 Integral vs. Differential Spectra

There are two different photon spectra types represented here. The first, the *Integral Photon Spectrum*, represents the total number of photons emitted within a particular energy bin per unit time. It is a measure of the *overall intensity* of the source within that bin's energy range. Its units are cm^2/s , or $\text{cm}^2 \cdot \text{s}$. The second type, the *Differential Photon Spectrum*, represents the rate of photon emission in a specific energy bin per unit energy, in this case, the MeV. It represents the *energy distribution of the emitted photons*. Its units are $\text{cm}^2/\text{MeV}/\text{s}$, or $\text{cm}^2 \cdot \text{MeV} \cdot \text{s}$.

2.3 Effects of Trapped Particle Radiation on Spacecraft Components

The following is from the SPENVIS trapped particle radiation documentation. I reproduce it here because it is a concise statement of why the following results are critically important to orbit determination.[\[6\]](#)

Effects of trapped particle radiation on spacecraft and components

Due to their large energy coverage, trapped particles cause a variety of effects in spacecraft, components and biological systems.

Low energy electrons contribute to spacecraft surface charging. High energy electrons injected and accelerated through the magnetotail can cause dielectric charge buildup deep inside geosynchronous spacecraft which may lead in turn to destructive arcing. Inner and outer belt electrons also contribute to ionising doses through direct energy deposition and bremsstrahlung effects.

High energy protons in the inner radiation belt are the main contributors to ionising dose deposition in shielded components. They also dominate Single Event Upset (SEU) rates at low altitudes and latitudes, where cosmic rays and solar energetic particles are effectively shielded by the geomagnetic field. Lower energy protons (up to 10 MeV) contribute to Non-Ionising Energy Loss (NIEL) dose which affects Charged-Coupled Devices (CCD) and other detectors; unshielded detectors can be affected even in the outer belt, where <1 MeV protons are present.

3 Orbits

Four different orbits are presented in the following sections. Three are geocentric. one heliocentric. One of the geocentric orbits, the Medium Earth Orbit (MEO), was provided by a potential contractor.

MEO Orbit

Long term stable, medium earth orbit. MEOs are generally used for Global Positioning Satellites. MEO orbits are enveloped by the Van Allen radiation belts, exposing them to high levels of trapped proton and electron bombardment.

Orbit Description

ϵ	Eccentricity:	0.0
i	Inclination:	80.0
P	Period:	711 mins
a	Semimajor Axis:	26,000 km
ω	Argument of Perigee:	270°
Ω	RAAN:	180°
Perigee:	20,000 km	
Apogee:	3.15 R_e	
	20,000 km	
	3.15 R_e	

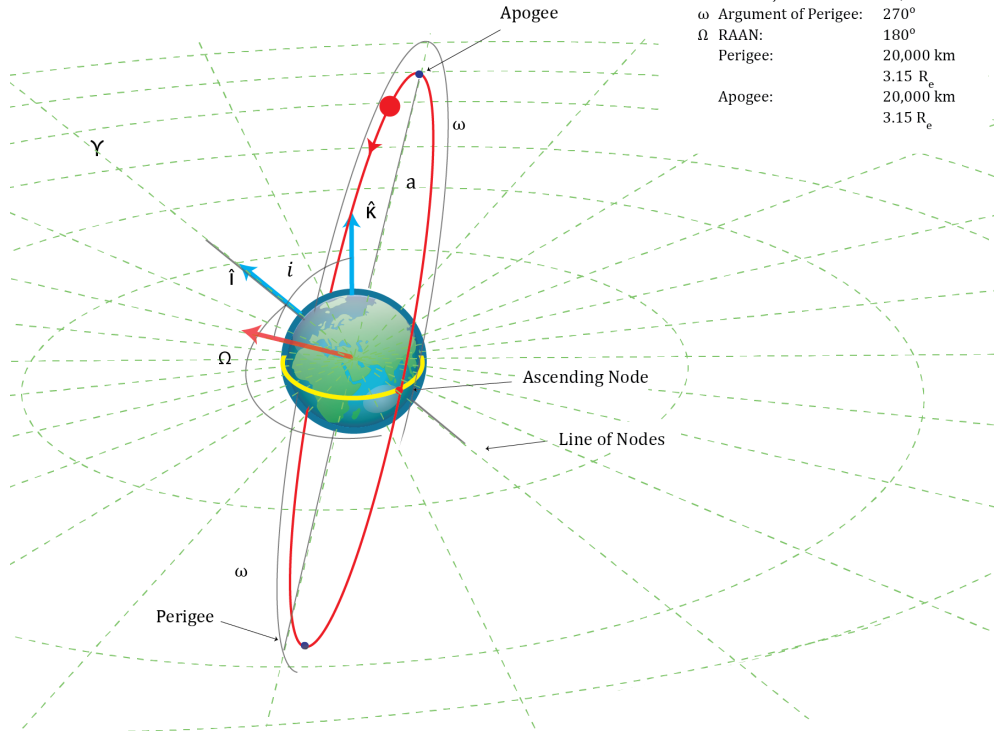


Figure 1: The Medium Earth Orbit and description.

Another, the Molniya orbit, is a common Highly Elliptical Orbit (HEO) type that is frequently considered for astronomical imaging missions. The third, the P/2 HEO, is an orbit utilized by the Transiting Exoplanet Survey Satellite (TESS) mission, a mission similar to Pearl. The heliocentric orbit, called the Earth Trailing Orbit (ETO), is one that was first used by the Spitzer Space Telescope.

3.1 MEO-Type Orbits

A potential contractor has strongly recommended one of two Medium Earth Orbit trajectories; either a MEO with a 70 to 80 degree inclination, or an Equatorial MEO (EMEO).

3.1.1 The Medium Earth Orbit

Figure 1 is a diagram of the MEO orbit at a 70° inclination and with contractor specified orbital parameters. It is fully circular ($\epsilon = 0$) with both apogee and perigee at 3.15 Earth radii. MEO orbits are typically used for global positioning and communications satellites, and complete roughly two orbits in a 24 hour period. They are highly unusual orbits to be considered for astronomical imaging missions for a number of reasons, including exposure to thermal effects from Earth's heat radiation, solar radiation pressure trajectory perturbations, and insufficient integration times due to the short orbital period. High energy trapped particles are problematic in this orbit as well. Figure 2 shows a plot of the intersection of the orbit with the high energy proton and electron regions of the Van Allen Belts (VAB).

3.1.2 The Equatorial Medium Earth Orbit

The EMEO trajectory is also circular, lies in the plane of the Earth's equator, and is fully embedded in both the Proton and Electron zones of the VAB: this is shown in Figure 3. Although in the lower energetic portion of the Proton region, continuous 24 hour exposure to a 10 MeV proton flux sums to a large total fluence over the lifetime of the mission.

The high energy electron situation is far worse: the satellite would be continuously exposed to a 10^5 MeV electron flux over the lifetime of the mission. Exposure to high energy electrons is now being looked at as the cause of 26 hard failures in eight satellites over a period of sixteen years. Satellites in these orbits are heavily shielded and use radiation hardened equipment to protect against the extreme high energy proton and electron environment.

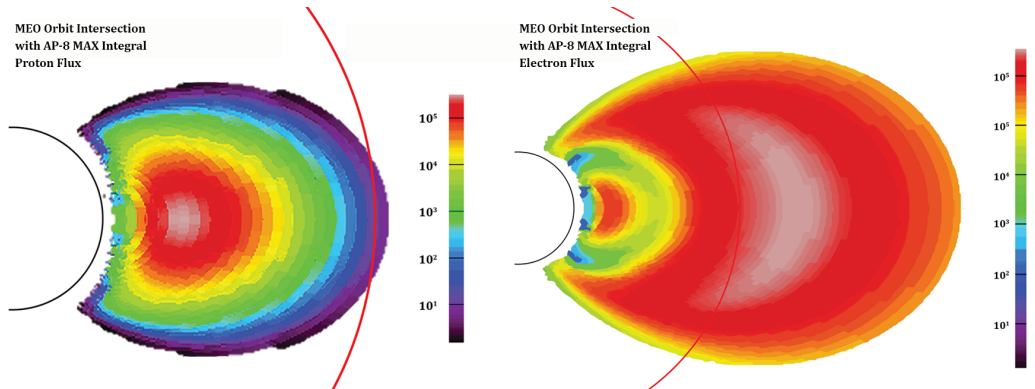


Figure 2: The MEO Orbital Intersection with the Van Allen proton and electron regions. Scale units are MeV per centimeter squared per second.

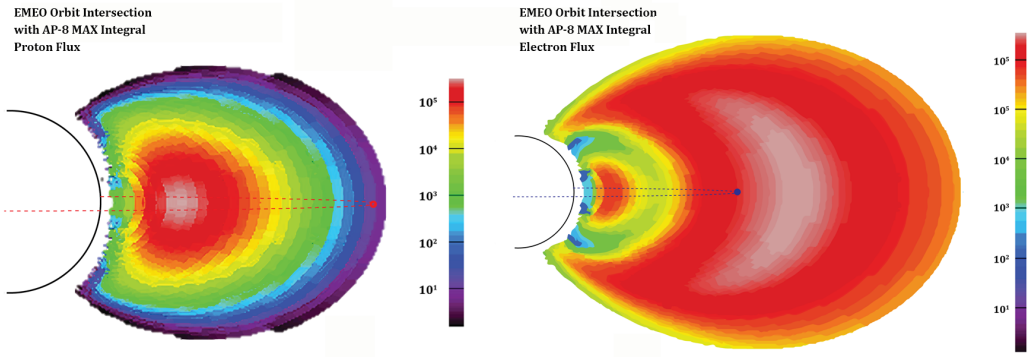


Figure 3: The EMEO Orbital Intersection with the Van Allen proton and electron regions. Scale units are MeV per centimeter squared per second.

3.2 Molniya Orbit

The Molniya orbit is named after the Russian word for lightning for its rapid passage through perigee. The orbit was originally designed for communications satellites and has a large dwell time at apogee over its hemisphere of interest. It has a relatively low ΔV to orbit, but has sizable station-keeping requirements.

Molniya Orbit

Lightning in Russian, named after the Molniya communications Satellite, the first to use the orbit in April 1965. The orbit crosses the proton and electron radiation belts at their most concentrated regions.

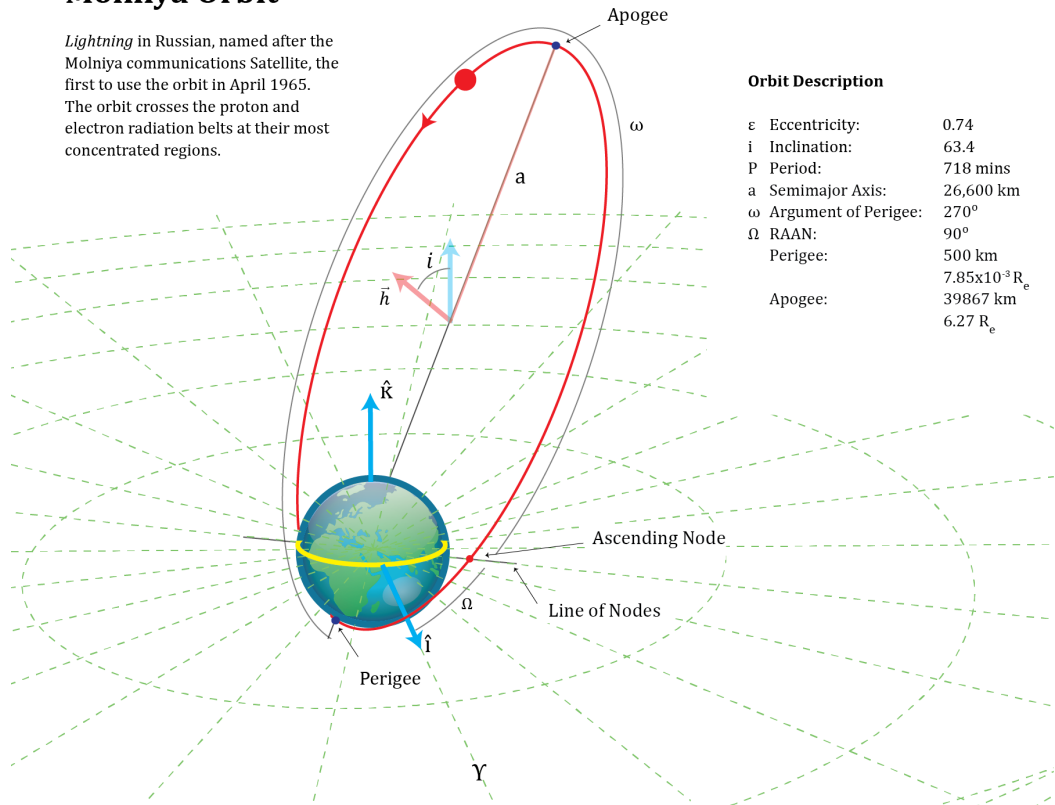


Figure 4: The Molniya orbit and orbit description.

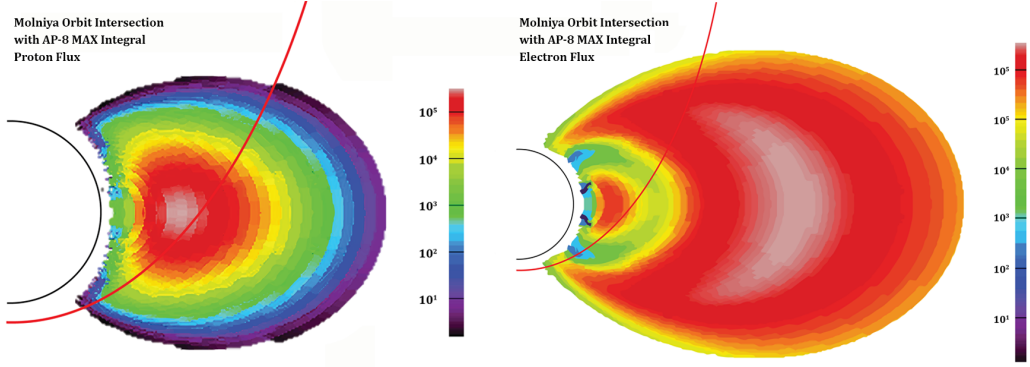


Figure 5: The Molniya Orbital Intersection with the Van Allen proton and electron regions. Scale units are MeV per centimeter squared per second.

Its rapid passage through perigee also makes communications with the satellite difficult, as a ground station must have steerable antennas to track the spacecraft, and rapid range changes cause variations in signal amplitude. The orbit also requires the satellite to pass through the VABs four times per day. The orbit is illustrated in Figure 4, and its intersection with the Van Allen proton and electron regions is shown in Figure 5.

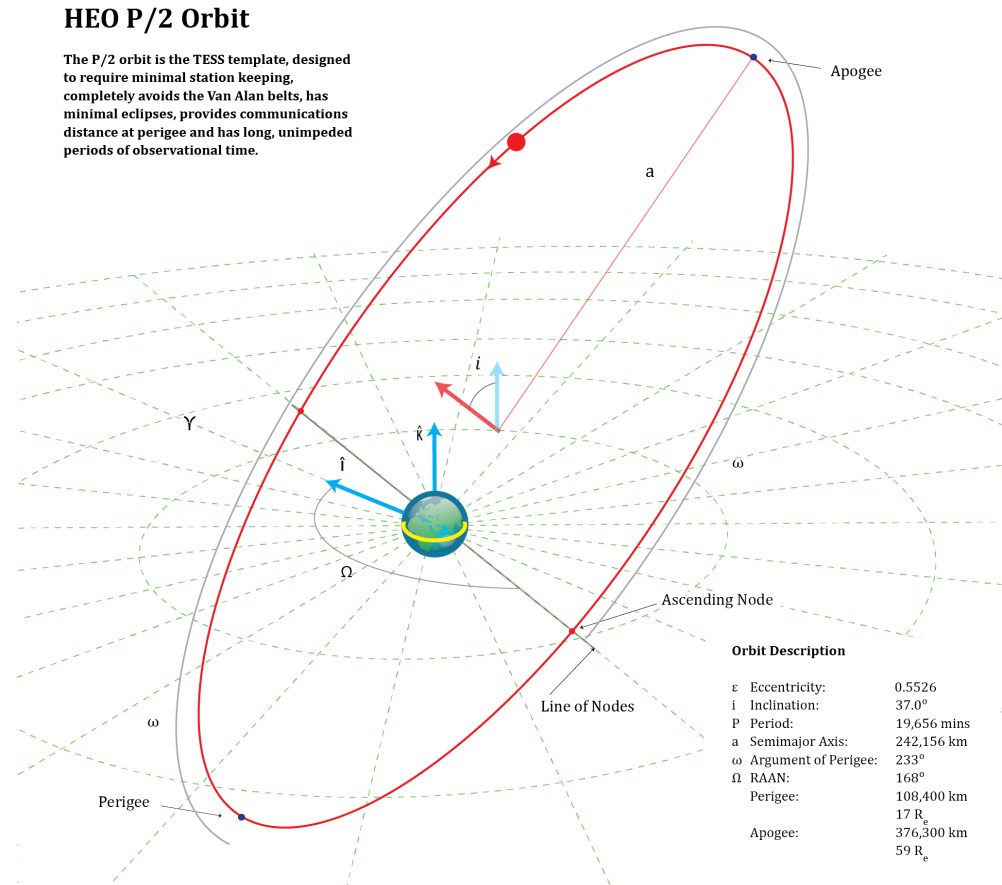


Figure 6: The P/2 HEO TESS Orbit diagram and description.

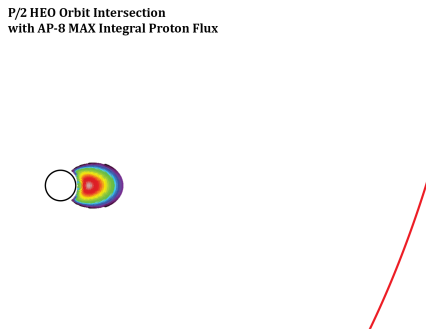


Figure 7: The P/2 HEO TESS Orbital Intersection, or lack thereof, with the Van Allen proton regions.

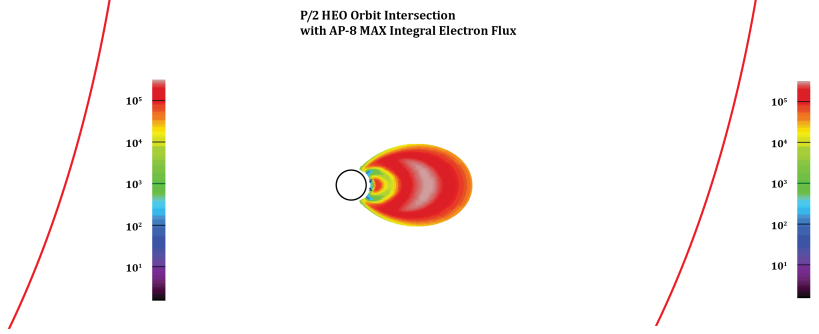


Figure 8: The P/2 HEO TESS Orbital Intersection, or lack thereof, with the Van Allen electron regions.

3.3 P/2-HEO Orbit (TESS)

The P/s HEO orbit is well suited for exoplanet imaging missions. It has been used for this type of mission before: The Transiting Exoplanet Survey Satellite, or TESS.

The P/2-HEO orbit is a highly elliptical, high earth orbit in 2:1 resonance with the moon, shown in Figure 6. First studied by McGiffin and Mathews in 2001, it was eventually utilized for the Transiting Exoplanet Survey Satellite mission. Its perigee lies above GEO altitude, its apogee is beyond the moon's orbital radius, and it completely avoids the Van Allen Belts (Figures 8 and 7). Through clever design, it balances solar and lunar perturbations, creating a highly stable orbit with a lifetime of decades while virtually eliminating the need for station keeping.

Its perigee altitude is ideal for communications, and its apogee provides long, unobstructed views that easily accommodate long imaging integration times. It also has a large trade space of possible designs to accommodate mission requirements. These designs all require relatively modest ΔV , between 175 m/s and 400 m/s, depending on the specific orbit and launch site.^[3] For more detail on the TESS orbit, see the internal memo 'The Argument for the P/2 HEO Orbit'.

3.4 Earth-Trailing Orbit

3.4.1 Description

Essentially, the Earth Trailing Orbit (ETO) is the Earth's orbit, but with a smaller eccentricity ($e_{ETO} = 0.011$ vs $e_{Earth} = 0.0167$), a longer period ($P_{ETO} = 372.2$ days vs $P_{Earth} = 365.2$ days), and an inclination of 1.13° to the plane of the Earth's orbit. The satellite trails the earth, and recedes at approximately 0.12 AU per year. The orbit diagram is shown in Figure 9.

The Spitzer infrared space telescope and the Kepler Planet-Finder space telescope both used the ETO. The benefits of the ETO orbit include avoiding the gravitational and torque effects of earth orbit and avoiding Earth occultations.

Advantages of the ETO Orbit

- Absence of Eclipses;
- Stable Thermal Configuration;
- High Observing Efficiency;
- No need for station keeping.

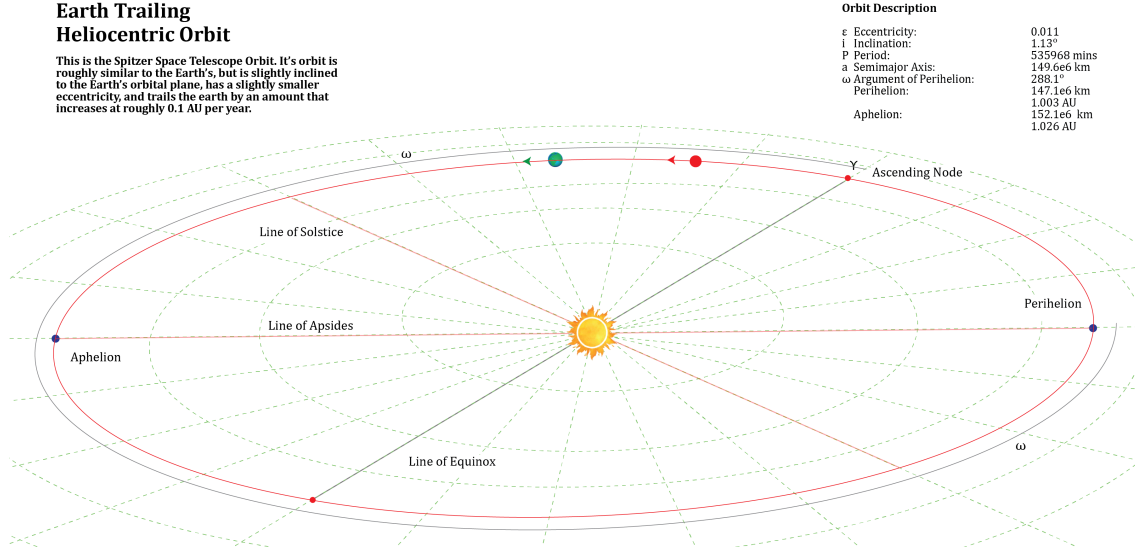


Figure 9: The Earth Trailing Orbit and description.

Disadvantages of the ETO Orbit

- Power requirement for communication increases as satellite recedes;
- Launch to orbit ΔV is in excess of 4,000 m/s [1];
- Orbit is outside of the Magnetosphere, leading to:
 - Greater susceptibility to solar proton storms;
 - Higher quiescent galactic cosmic flux rate.

4 Orbit Radiation

4.1 A few Notes

4.1.1 Note on ETO Radiation Data

The Earth-Trailing Orbit (ETO) cannot easily be modeled with SPENVIS; in order to do so, the heliocentric parameters would need to be expressed in geocentric terms, producing epicycles and deferents that would make Ptolemy cringe. Therefore, data from the National Oceanic and Atmospheric Administration's (NOAA) Geostationary Operational Environmental Satellites, R Series (GEOS-R), can be used to provide insight into the nature of the ETO Solar Energetic Particle (SEP) environment.

Previous generation GEOS satellites carry a Space Environment Monitor (SEM) instrumentation package which includes an Energetic Particle Sensor (EPS) instrument. The EPS onboard GEOS-13 through GEOS-15 measures protons from 80 keV to 100s of MeV. In addition, GEOS-4 through GEOS-15 included a High Energy Proton and Alpha Detector (HEPAD) instrument which measures high energy proton fluxes above 350 MeV in four broadband channels.[2] The current generation of GEOS satellites, starting with GEOS-16, have replaced the original SEM package with the new five instrument Space environment In-Situ Suite (SEISS) package. Two of these instruments are the Solar and Galactic Proton Sensor (SGPS) units, facing in opposite directions. SGPS measures protons with energies from 1 to >500 MeV in fourteen channels. Solar Proton Events (SPEs) occurring in July and September of 2017 enables cross calibration between the EPS and SGPS instruments.[2]

In the 2022 Astronomy & Astrophysics article 'Annual Integral Solar Proton Fluences' [4], the authors use data from GEOS Satellites to provide solar proton fluences from 1984 to 2019. These fluences show the expected variability resulting from the 11-year solar cycle, and are thus extremely useful for evaluating the ETO's potential SEP exposure.

4.1.2 Notes on Simulations

All Trapped Proton Fluxes and Fluences simulations and all Solar Particle Fluences simulations were run with the same parameters. No simulations took into account spaceship shielding to simplify the simulation setup.

Trapped Proton Fluxes and Fluences These simulations examine the Van Allen Belt proton flux along the spacecraft's trajectory, and were run using the standard AP8/AE8 model set at solar maxima. The internal magnetic field model is GSFC 12/66 120, update 1970.[6] Trajectory parameters are as shown on the orbit illustrations, for a one year mission duration with science orbit commencing 00:00:00 01 January 2025.

Solar Particle Fluences Solar particle modeling was conducted with SPENVIS Emission of Solar Protons (ESP), for total fluence using worst case events.[5] All available ions, from Hydrogen to Uranium, were selected. Magnetosphere shielding was set as Eccentric Dipole/Quiet Magnetosphere/Unchanged Magnetic Moment/All Arrival Directions. Confidence level that fluences would not be exceeded was set to 95%. Trajectory parameters are as shown on the orbit illustrations, for a one year mission duration with science orbit starting 00:00:00 January 1st 2025.

MEO Integral Proton Spectra				
Energy (MeV)	Total Mission Average Flux (/cm ² /MeV/s)	Total Mission Fluence (/cm ² /MeV)	Segment One Average Flux (/cm ² /MeV/s)	Segment One Fluence (/cm ² /MeV)
0.10	2.100E+07	6.6230B+14	2.100E+07	6.6230B+14
0.15	1.539E+07	4.8519E+14	1.539E+07	4.8519E+14
0.20	1.137E+07	3.5846E+14	1.137E+07	3.5846E+14
0.30	6.597E+06	2.0805B+14	6.597E+06	2.0805B+14
0.40	3.890E+06	1.2266B+14	3.890E+06	1.2266B+14
0.50	2.311E+06	7.2880E+13	2.311E+06	7.2880E+13
0.60	1.385E+06	4.3684E+13	1.385E+06	4.3684E+13
0.70	8.544E+05	2.6943B+13	8.544E+05	2.6943B+13
1.00	1.899E+05	5.9875E+12	1.899E+05	5.9875E+12
1.50	1.880E+04	5.9288E+11	1.880E+04	5.9288E+11
2.00	1.896E+03	5.9792E+10	1.896E+03	5.9792E+10
3.00	8.370E+01	2.6396E+09	8.370E+01	2.6396E+09
4.00	3.728E+00	1.1758B+08	3.728E+00	1.1758B+08
5.00	1.806E-01	5.6953B+06	1.806E-01	5.6953B+06
6.00	1.365E-02	4.3058E+05	1.365E-02	4.3058E+05
7.00	0.0000E+00	0.0000E+00	0.0000E+00	0.0000E+00
10.00	0.0000E+00	0.0000E+00	0.0000E+00	0.0000E+00
15.00	0.0000E+00	0.0000E+00	0.0000E+00	0.0000E+00
20.00	0.0000E+00	0.0000E+00	0.0000E+00	0.0000E+00
30.00	0.0000E+00	0.0000E-00	0.0000E+00	0.0000E-00
40.00	0.0000E+00	0.0000E+00	0.0000E+00	0.0000E+00
50.00	0.0000E+00	0.0000E+00	0.0000E+00	0.0000E+00
60.00	0.0000E+00	0.0000E+00	0.0000E+00	0.0000E+00
70.00	0.0000E+00	0.0000E+00	0.0000E+00	0.0000E+00
100.00	0.0000E+00	0.0000E+00	0.0000E+00	0.0000E+00
150.00	0.0000E+00	0.0000E+00	0.0000E+00	0.0000E+00
200.00	0.0000E+00	0.0000E+00	0.0000E+00	0.0000E+00
300.00	0.0000E+00	0.0000E+00	0.0000E+00	0.0000E+00
400.00	0.0000E+00	0.0000E+00	0.0000E+00	0.0000E+00

Figure 10: The MEO Solar Maxima trapped proton fluxes and fluences, Integral Spectra.

MEO Differential Proton Spectra				
Energy (MeV)	Total Mission Average Flux (/cm ² /MeV/s)	Total Mission Fluence (/cm ² /MeV)	Segment One Average Flux (/cm ² /MeV/s)	Segment One Fluence (/cm ² /MeV)
0.10	1.283E+08	4.046E+15	1.283E+08	4.046E+15
0.15	9.635E+07	3.038E+15	9.635E+07	3.038E+15
0.20	6.948E+07	2.191E+15	6.948E+07	2.191E+15
0.30	3.739E+07	1.179E+15	3.739E+07	1.179E+15
0.40	2.143E+07	6.759E+14	2.143E+07	6.759E+14
0.50	1.252E+07	3.949E+14	1.252E+07	3.949E+14
0.60	7.283E+06	2.297E+14	7.283E+06	2.297E+14
0.70	4.535E+06	1.430E+14	4.535E+06	1.430E+14
1.00	1.513E+06	4.770E+13	1.513E+06	4.770E+13
1.50	1.880E+05	5.928E+12	1.880E+05	5.928E+12
2.00	2.314E+04	7.298E+11	2.314E+04	7.298E+11
3.00	9.461E+02	2.984E+10	9.461E+02	2.984E+10
4.00	4.176E+01	1.317E+09	4.176E+01	1.317E+09
5.00	1.857E+00	5.858E+07	1.857E+00	5.858E+07
6.00	9.030E-02	2.848E+06	9.030E-02	2.848E+06
7.00	1.024E-02	3.229E+05	1.024E-02	3.229E+05
10.00	0.0000E+00	0.0000E+00	0.0000E+00	0.0000E+00
15.00	0.0000E+00	0.0000E+00	0.0000E+00	0.0000E+00
20.00	0.0000E+00	0.0000E+00	0.0000E+00	0.0000E+00
30.00	0.0000E+00	0.0000E+00	0.0000E+00	0.0000E+00
40.00	0.0000E+00	0.0000E+00	0.0000E+00	0.0000E+00
50.00	0.0000E+00	0.0000E+00	0.0000E+00	0.0000E+00
60.00	0.0000E+00	0.0000E+00	0.0000E+00	0.0000E+00
70.00	0.0000E+00	0.0000E+00	0.0000E+00	0.0000E+00
100.00	0.0000E+00	0.0000E+00	0.0000E+00	0.0000E+00
150.00	0.0000E+00	0.0000E+00	0.0000E+00	0.0000E+00
200.00	0.0000E+00	0.0000E+00	0.0000E+00	0.0000E+00
300.00	0.0000E+00	0.0000E+00	0.0000E+00	0.0000E+00
400.00	0.0000E+00	0.0000E+00	0.0000E+00	0.0000E+00

Figure 11: The MEO Solar Maxima trapped proton fluxes and fluences, Differential Spectra.

4.2 MEO Orbit Simulations

4.2.1 Trapped Proton Fluxes and Fluences

I have only shown results for the MEO orbit, as the high energy electron exposure for the EMEO orbit immediately disqualifies it from consideration. Figure 10 above shows the MEO Orbit AP8 SPENVIS Integral Proton Spectra output; Figure 11 above shows the AP8 SPENVIS Differential Proton Spectra output.

4.2.2 Solar Particle Fluences

The MEO Orbit solar particle spectrum is shown in Figure 16.

4.3 Molniya Orbit Simulations

4.3.1 Trapped Proton Fluxes and Fluences

Figure 12 below shows the Molniya orbit AP8 SPENVIS Integral Proton Spectra output; Figure 13 below shows the AP8 SPENVIS Differential Proton Spectra output.

4.3.2 Solar Particle Fluences

The Molniya Orbit solar particle spectrum is shown in Figure 17.

Molniya Integral Proton Spectra				
Energy (MeV)	Total Mission Average Flux (/cm^2/MeV/s)	Total Mission Fluence (/cm^2/MeV)	Segment One Average Flux (/cm^2/MeV/s)	Segment One Fluence (/cm^2/MeV)
0.10	8.615E+06	2.717E+14	8.615E+06	2.717E+14
0.15	6.967E+06	2.197E+14	6.967E+06	2.197E+14
0.20	5.702E+06	1.798E+14	5.702E+06	1.798E+14
0.30	4.124E+06	1.301E+14	4.124E+06	1.301E+14
0.40	3.057E+06	9.641E+13	3.057E+06	9.641E+13
0.50	2.376E+06	7.494E+13	2.376E+06	7.494E+13
0.60	1.878E+06	5.923E+13	1.878E+06	5.923E+13
0.70	1.533E+06	4.835E+13	1.533E+06	4.835E+13
1.00	8.938E+05	2.819E+13	8.938E+05	2.819E+13
1.50	4.523E+05	1.427E+13	4.523E+05	1.427E+13
2.00	2.623E+05	8.271E+12	2.623E+05	8.271E+12
3.00	1.383E+05	4.360E+12	1.383E+05	4.360E+12
4.00	8.134E+04	2.565E+12	8.134E+04	2.565E+12
5.00	5.331E+04	1.681E+12	5.331E+04	1.681E+12
6.00	3.589E+04	1.132E+12	3.589E+04	1.132E+12
7.00	2.528E+04	7.971E+11	2.528E+04	7.971E+11
10.00	9.873E+03	3.114E+11	9.873E+03	3.114E+11
15.00	2.905E+03	9.161E+10	2.905E+03	9.161E+10
20.00	1.311E+03	4.133E+10	1.311E+03	4.133E+10
30.00	1.736E+10	1.736E+10	1.736E+10	1.736E+10
40.00	1.192E+10	1.192E+10	1.192E+10	1.192E+10
50.00	2.657E+02	8.379E+09	2.657E+02	8.379E+09
60.00	2.129E+02	6.714E+09	2.129E+02	6.714E+09
70.00	1.770E+02	5.583E+09	1.770E+02	5.583E+09
100.00	1.067E+02	3.363E+09	1.067E+02	3.363E+09
150.00	5.166E+01	1.629E+09	5.166E+01	1.629E+09
200.00	2.538E+01	8.003E+08	2.538E+01	8.003E+08
300.00	8.019E+00	2.529E+08	8.019E+00	2.529E+08
400.00	2.585E+00	8.153E+07	2.585E+00	8.153E+07

Figure 12: The Molniya Solar Maxima trapped proton fluxes and fluences, Integral Spectra.

Molniya Differential Proton Spectra				
Energy (MeV)	Total Mission Average Flux (/cm^2/MeV/s)	Total Mission Fluence (/cm^2/MeV)	Segment One Average Flux (/cm^2/MeV/s)	Segment One Fluence (/cm^2/MeV)
0.10	3.680E+07	1.160E+15	3.680E+07	1.160E+15
0.15	2.913E+07	9.187E+14	2.913E+07	9.187E+14
0.20	2.212E+07	6.977E+14	2.212E+07	6.977E+14
0.30	1.322E-07	4.170E+14	1.322E-07	4.170E+14
0.40	8.739E-06	2.756E+14	8.739E-06	2.756E+14
0.50	5.896E+06	1.859E+14	5.896E+06	1.859E+14
0.60	4.216E-06	1.330E+14	4.216E-06	1.330E+14
0.70	3.120E+06	9.840E+13	3.120E+06	9.840E+13
1.00	1.663E-06	5.245E+13	1.663E-06	5.245E+13
1.50	6.315E+05	1.992E+13	6.315E+05	1.992E+13
2.00	2.948E+05	9.296E+12	2.948E+05	9.296E+12
3.00	9.046E+04	2.853E+12	9.046E+04	2.853E+12
4.00	4.248E+04	1.340E+12	4.248E+04	1.340E+12
5.00	2.273E+04	7.167E+11	2.273E+04	7.167E+11
6.00	1.402E-04	4.420E+11	1.402E+04	4.420E+11
7.00	9.242E-03	2.915E+11	9.242E+03	2.915E-11
10.00	3.732E+03	1.177E+11	3.732E-03	1.177E-11
15.00	8.562E+02	2.700E+10	8.562E+02	2.700E+10
20.00	2.379E+02	7.503E+09	2.379E-02	7.503E+09
30.00	4.664E+01	1.471E+09	4.664E-01	1.471E+09
40.00	1.424E+01	4.491E+08	1.424E-01	4.491E+08
50.00	8.254E+00	2.603E+08	8.254E+00	2.603E+08
60.00	4.433E+00	1.398E+08	4.433E+00	1.398E+08
70.00	3.275E+00	1.033E+08	3.275E+00	1.033E+08
100.00	1.879E+00	5.925E+07	1.879E+00	5.925E+07
150.00	8.128E-01	2.563E+07	8.128E-01	2.563E+07
200.00	4.084E-01	1.288E+07	4.084E-01	1.288E+07
300.00	1.140E-01	3.594E+06	1.140E-01	3.594E+06
400.00	0.000E+00	0.000E+00	0.000E+00	0.000E+00

Figure 13: The Molniya Solar Maxima trapped proton fluxes and fluences, Differential Spectra.

P/2 HEO Integral Proton Spectra				
Energy (MeV)	Total Mission Average Flux (/cm ² /MeV/s)	Total Mission Fluence (/cm ² /MeV)	Segment One Average Flux (/cm ² /MeV/s)	Segment One Fluence (/cm ² /MeV)
0.10	1.260E+04	3.974E+11	1.260E+04	3.974E+11
0.15	6.481E+03	2.044E+11	6.481E+03	2.044E+11
0.20	3.343E+03	1.054E+11	3.343E+03	1.054E+11
0.30	1.193E+03	3.762E+10	1.193E+03	3.762E+10
0.40	4.272E+02	1.347E+10	4.272E+02	1.347E+10
0.50	1.597E+02	5.036E+09	1.597E+02	5.036E+09
0.60	6.007E+01	1.894E+09	6.007E+01	1.894E+09
0.70	2.263E+01	7.137E+08	2.263E+01	7.137E+08
1.00	1.286E+00	4.056E+07	1.286E+00	4.056E+07
1.50	1.532E-02	4.831E+05	1.532E-02	4.831E+05
2.00	0.000E+00	0.000E+00	0.000E+00	0.000E+00
3.00	0.000E+00	0.000E+00	0.000E+00	0.000E+00
4.00	0.000E+00	0.000E+00	0.000E+00	0.000E+00
5.00	0.000E+00	0.000E+00	0.000E+00	0.000E+00
6.00	0.000E+00	0.000E+00	0.000E+00	0.000E+00
7.00	0.000E+00	0.000E+00	0.000E+00	0.000E+00
10.00	0.000E+00	0.000E+00	0.000E+00	0.000E+00
15.00	0.000E+00	0.000E+00	0.000E+00	0.000E+00
20.00	0.000E+00	0.000E+00	0.000E+00	0.000E+00
30.00	0.000E+00	0.000E+00	0.000E+00	0.000E+00
40.00	0.000E+00	0.000E+00	0.000E+00	0.000E+00
50.00	0.000E+00	0.000E+00	0.000E+00	0.000E+00
60.00	0.000E+00	0.000E+00	0.000E+00	0.000E+00
70.00	0.000E+00	0.000E+00	0.000E+00	0.000E+00
100.00	0.000E+00	0.000E+00	0.000E+00	0.000E+00
150.00	0.000E+00	0.000E+00	0.000E+00	0.000E+00
200.00	0.000E+00	0.000E+00	0.000E+00	0.000E+00
300.00	0.000E+00	0.000E+00	0.000E+00	0.000E+00
400.00	0.000E+00	0.000E+00	0.000E+00	0.000E+00

P/2 HEO Differential Proton Spectra				
Energy (MeV)	Total Mission Average Flux (/cm ² /MeV/s)	Total Mission Fluence (/cm ² /MeV)	Segment One Average Flux (/cm ² /MeV/s)	Segment One Fluence (/cm ² /MeV)
0.1	1.522E+05	4.800E+12	1.522E+05	4.800E+12
0.15	9.258E+04	2.920E+12	9.258E+04	2.920E+12
0.20	4.901E+04	1.545E+12	4.901E+04	1.545E+12
0.30	1.458E+04	4.598E+11	1.458E+04	4.598E+11
0.40	5.166E+03	1.629E+11	5.166E+03	1.629E+11
0.50	1.835E+03	5.788E+10	1.835E+03	5.788E+10
0.60	6.853E+02	2.161E+10	6.853E+02	2.161E+10
0.70	2.986E+02	9.416E+09	2.986E+02	9.416E+09
1.00	4.542E+01	1.433E+09	4.542E+01	1.433E+09
1.50	1.286E+00	4.056E+07	1.286E+00	4.056E+07
2.00	2.042E-02	6.441E+05	2.042E-02	6.441E+05
3.00	0.000E+00	0.000E+00	0.000E+00	0.000E+00
4.00	0.000E+00	0.000E+00	0.000E+00	0.000E+00
5.00	0.000E+00	0.000E+00	0.000E+00	0.000E+00
6.00	0.000E+00	0.000E+00	0.000E+00	0.000E+00
7.00	0.000E+00	0.000E+00	0.000E+00	0.000E+00
10.00	0.000E+00	0.000E+00	0.000E+00	0.000E+00
15.00	0.000E+00	0.000E+00	0.000E+00	0.000E+00
20.00	0.000E+00	0.000E+00	0.000E+00	0.000E+00
30.00	0.000E+00	0.000E+00	0.000E+00	0.000E+00
40.00	0.000E+00	0.000E+00	0.000E+00	0.000E+00
50.00	0.000E+00	0.000E+00	0.000E+00	0.000E+00
60.00	0.000E+00	0.000E+00	0.000E+00	0.000E+00
70.00	0.000E+00	0.000E+00	0.000E+00	0.000E+00
100.00	0.000E+00	0.000E+00	0.000E+00	0.000E+00
150.00	0.000E+00	0.000E+00	0.000E+00	0.000E+00
200.00	0.000E+00	0.000E+00	0.000E+00	0.000E+00
300.00	0.000E+00	0.000E+00	0.000E+00	0.000E+00
400.00	0.000E+00	0.000E+00	0.000E+00	0.000E+00

Figure 14: The P/2 HEO (TESS) Solar Maxima trapped proton fluxes and fluences, Integral Spectra.

Figure 15: The P/2 HEO (TESS) Solar Maxima trapped proton fluxes and fluences, Differential Spectra.

4.4 P/2 HEO TESS Orbit Simulations

4.4.1 Trapped Proton Fluxes and Fluences

Figure 14 above shows the P/2 HEO Orbit AP8 SPENVIS Integral Proton Spectra output; Figure 15 above shows the AP8 SPENVIS Differential Proton Spectra output.

4.4.2 Solar Particle Fluences

The P/2 HEO TESS solar particle spectrum is shown in Figure 18.

4.5 Earth Trailing Orbit Data

As the ETO is, by definition, outside the region of the Van Allen Belts, the only relevant radiation data concerns high energy solar particles. The following data is from the National Oceanic and Atmospheric Administration's (NOAA) Geostationary Operational Environmental Satellites, R Series (GEOS-R), as discussed in Section 4.1.1.

The chart shown in Figure 19 below shows annual integral solar fluences for the years 1984 - 2019, along with error values, in units of particles per cm^{-2} . Each column in the chart alternates between a fluence bin that begins at the given energy level indicated by the subscript, and an error value for that bin. On the right side of the chart is an ordering of the F_{10MeV} fluences by year (the green bars are meaningless here). The years 1989, 2000, 2001 and 2003 were the most active recent years in terms of solar particle events. A chart of solar proton events for the years 1976 through 2017 is presented in the appendix.

MEO Solar Proton Fluxes for Trajectory and at 1.0 AU				
	Fluence at Spacecraft		Model Fluence at 1.0 AU	
	Total Mission Fluence	Total Prediction Period		
Energy (MeV)	Integral (cm^-2)	Differential (cm^-2 MeV^-1)	Integral (cm^-2)	Differential (cm^-2 MeV^-1)
0.10	8.319E+11	5.548E+12	1.178E+12	7.975E+12
0.11	7.801E+11	4.811E+12	1.103E+12	6.915E+12
0.12	7.352E+11	4.169E+12	1.039E+12	5.993E+12
0.14	6.611E+11	3.234E+12	9.352E+11	4.649E+12
0.16	6.031E+11	2.573E+12	8.535E+11	3.698E+12
0.18	5.563E+11	2.104E+12	7.873E+11	3.025E+12
0.20	5.176E+11	1.759E+12	7.325E+11	2.528E+12
0.22	4.851E+11	1.500E+12	6.862E+11	2.156E+12
0.25	4.444E+11	1.212E+12	6.286E+11	1.742E+12
0.28	4.112E+11	1.001E+12	5.817E+11	1.439E+12
0.32	3.752E+11	7.979E+11	5.308E+11	1.147E+12
0.35	3.529E+11	6.859E+11	4.992E+11	9.859E+11
0.40	3.200E+11	5.493E+11	4.556E+11	7.896E+11
0.45	2.971E+11	4.493E+11	4.202E+11	6.459E+11
0.50	2.765E+11	3.256E+11	3.337E+11	3.674E+11
0.55	2.591E+11	3.025E+11	3.663E+11	4.606E+11
0.63	2.360E+11	2.556E+11	3.337E+11	3.674E+11
0.71	2.174E+11	2.086E+11	3.075E+11	2.999E+11
0.80	2.004E+11	1.706E+11	2.833E+11	2.452E+11
0.90	1.849E+11	1.397E+11	2.614E+11	2.008E+11
1.00	1.720E+11	1.168E+11	2.432E+11	1.679E+11
1.10	1.612E+11	9.933E+10	2.278E+11	1.428E+11
1.20	1.520E+11	8.608E+10	2.146E+11	1.237E+11
1.40	1.367E+11	6.677E+10	1.931E+11	9.598E+10
1.60	1.247E+11	5.312E+10	1.762E+11	7.636E+10
1.80	1.150E+11	4.345E+10	1.626E+11	6.246E+10
2.00	1.071E+11	3.632E+10	1.512E+11	5.220E+10
2.20	1.003E+11	3.097E+10	1.417E+11	4.452E+10
2.50	9.193E+10	2.502E+10	1.298E+11	3.596E+10
2.80	8.492E+10	2.169E+10	1.201E+11	3.117E+10
3.20	7.665E+10	1.969E+10	1.082E+11	2.830E+10
3.50	7.105E+10	1.764E+10	1.001E+11	2.536E+10
4.00	6.319E+10	1.378E+10	8.898E+10	1.981E+10
4.50	5.699E+10	1.101E+10	8.024E+10	1.583E+10
5.00	5.185E+10	9.574E+09	7.315E+10	1.376E+10
5.50	4.732E+10	8.546E+09	6.648E+10	1.228E+10
6.30	4.127E+10	6.569E+09	5.801E+10	9.442E+09
7.10	3.649E+10	5.381E+09	5.137E+10	7.734E+09
8.00	3.208E+10	4.421E+09	4.498E+10	6.355E+09
9.00	2.815E+10	3.441E+09	3.946E+10	4.946E+09
10.00	2.498E+10	2.890E+09	3.509E+10	4.154E+09
11.00	2.229E+10	2.488E+09	3.115E+10	3.576E+09
12.00	2.002E+10	2.057E+09	2.794E+10	2.957E+09
14.00	1.647E+10	1.498E+09	2.304E+10	2.154E+09
16.00	1.381E+10	1.154E+09	1.932E+10	1.658E+09
18.00	1.177E+10	8.959E+08	1.641E+10	1.288E+09
20.00	1.015E+10	7.161E+08	1.417E+10	1.029E+09
22.00	8.846E+09	5.914E+08	1.229E+10	8.501E+08
25.00	7.295E+09	4.426E+08	1.015E+10	6.362E+08
28.00	6.111E+09	3.462E+08	8.472E+09	4.977E+08
32.00	4.919E+09	2.499E+08	6.810E+09	3.592E+08
35.00	4.242E+09	2.014E+08	5.859E+09	2.894E+08
40.00	3.371E+09	1.470E+08	4.642E+09	2.113E+08
45.00	2.731E+09	1.090E+08	3.746E+09	1.567E+08
50.00	2.252E+09	8.275E+07	3.075E+09	1.189E+08
55.00	1.883E+09	6.485E+07	2.557E+09	9.322E+07
63.00	1.443E+09	4.514E+07	1.945E+09	6.488E+07
71.00	1.134E+09	3.213E+07	1.519E+09	4.618E+07
80.00	8.863E+08	2.294E+07	1.175E+09	3.297E+07
90.00	6.905E+08	1.622E+07	9.034E+08	2.331E+07
100.00	5.515E+08	1.158E+07	7.088E+08	1.662E+07
110.00	4.516E+08	8.404E+06	5.711E+08	1.200E+07
120.00	3.771E+08	6.491E+06	4.688E+08	9.196E+06
140.00	2.702E+08	4.197E+06	3.260E+08	5.824E+06
160.00	2.005E+08	2.777E+06	2.359E+08	3.741E+06
180.00	1.534E+08	1.934E+06	1.763E+08	2.512E+06
200.00	1.201E+08	1.394E+06	1.354E+08	1.761E+06
220.00	9.576E+07	1.041E+06	1.059E+08	1.285E+06
250.00	6.964E+07	7.000E+05	7.584E+07	8.400E+05
280.00	5.183E+07	4.875E+05	5.550E+07	5.711E+05
320.00	3.606E+07	3.009E+05	3.836E+07	3.440E+05
350.00	2.830E+07	2.170E+05	2.994E+07	2.448E+05
400.00	1.948E+07	1.356E+05	2.070E+07	1.500E+05
450.00	1.390E+07	8.763E+04	1.494E+07	9.531E+04
500.00	1.041E+07	5.199E+04	1.117E+07	5.578E+04

Figure 16: The MEO Solar Particle Emission Spectrum.

Molniya Solar Proton Fluxes for Trajectory and at 1.0 AU				
	Fluence at Spacecraft		Model Fluence at 1.0 AU	
	Total Mission Fluence	Total Prediction Period		
Energy (MeV)	Integral (cm^-2)	Differential (cm^-2 MeV^-1)	Integral (cm^-2)	Differential (cm^-2 MeV^-1)
0.10	9.555E+11	6.373E+12	1.178E+12	7.975E+12
0.11	8.960E+11	5.526E+12	1.103E+12	6.915E+12
0.12	8.444E+11	4.789E+12	1.039E+12	5.993E+12
0.14	7.594E+11	3.715E+12	9.352E+11	4.649E+12
0.16	6.927E+11	2.955E+12	8.535E+11	3.698E+12
0.18	6.390E+11	2.417E+12	7.873E+11	3.025E+12
0.20	5.946E+11	2.020E+12	7.325E+11	2.528E+12
0.22	5.572E+11	1.723E+12	6.862E+11	2.156E+12
0.25	5.104E+11	1.392E+12	6.286E+11	1.742E+12
0.28	4.723E+11	1.150E+12	5.817E+11	1.439E+12
0.32	4.310E+11	9.165E+11	5.308E+11	1.147E+12
0.35	4.054E+11	7.878E+11	4.992E+11	9.859E+11
0.40	3.699E+11	6.310E+11	4.556E+11	7.896E+11
0.45	3.413E+11	5.161E+11	4.202E+11	6.459E+11
0.50	3.176E+11	4.314E+11	3.910E+11	5.398E+11
0.55	2.976E+11	3.681E+11	3.663E+11	4.606E+11
0.63	2.711E+11	2.936E+11	3.337E+11	3.674E+11
0.71	2.498E+11	2.397E+11	3.075E+11	2.999E+11
0.80	2.302E+11	1.960E+11	2.833E+11	2.452E+11
0.90	2.124E+11	1.605E+11	2.614E+11	2.008E+11
1.00	1.976E+11	1.341E+11	2.432E+11	1.679E+11
1.10	1.852E+11	1.141E+11	2.278E+11	1.428E+11
1.20	1.746E+11	9.888E+10	2.146E+11	1.237E+11
1.40	1.570E+11	7.670E+10	1.931E+11	9.598E+10
1.60	1.432E+11	6.102E+10	1.762E+11	7.636E+10
1.80	1.321E+11	4.991E+10	1.626E+11	6.246E+10
2.00	1.230E+11	4.171E+10	1.512E+11	5.220E+10
2.20	1.153E+11	3.558E+10	1.417E+11	4.452E+10
2.50	1.056E+11	2.874E+10	1.298E+11	3.596E+10
2.80	9.756E+10	3.117E+10	2.491E+10	1.201E+11
3.20	8.805E+10	2.261E+10	1.082E+11	2.830E+10
3.50	8.162E+10	2.027E+10	1.001E+11	2.536E+10
4.00	7.260E+10	1.583E+10	8.898E+10	1.981E+10
4.50	6.548E+10	1.265E+10	8.024E+10	1.583E+10
5.00	5.957E+10	1.100E+10	7.315E+10	1.376E+10
5.50	5.436E+10	9.816E+09	6.648E+10	1.228E+10
6.30	4.742E+10	7.545E+09	5.801E+10	9.442E+09
7.10	4.193E+10	6.180E+09	5.137E+10	7.734E+09
8.00	3.686E+10	5.078E+09	4.498E+10	6.355E+09
9.00	3.235E+10	4.946E+09	3.953E+10	3.946E+09
10.00	2.871E+10	3.319E+09	3.509E+10	4.154E+09
11.00	2.562E+10	2.858E+09	3.115E+10	3.576E+09
12.00	2.301E+10	2.363E+09	2.794E+10	2.957E+09
14.00	1.893E+10	1.721E+09	2.304E+10	2.154E+09
16.00	1.588E+10	1.325E+09	1.932E+10	1.658E+09
18.00	1.353E+10	1.029E+09	1.641E+10	1.288E+09
20.00	1.168E+10	8.225E+08	1.417E+10	1.029E+09
22.00	1.018E+10	6.793E+08	1.229E+10	8.501E+08
25.00	8.395E+09	5.084E+08	1.015E+10	6.362E+08
28.00	7.035E+09	3.977E+08	8.472E+09	4.377E+08
32.00	5.666E+09	2.871E+08	6.810E+09	3.592E+08
35.00	4.888E+09	2.314E+08	5.859E+09	2.894E+08
40.00	3.887E+09	1.692E+08	4.642E+09	2.113E+08
45.00	3.150E+09	1.257E+08	3.746E+09	1.567E+08
50.00	2.596E+09	9.557E+07	3.075E+09	1.189E+08
55.00	2.170E+09	7.506E+07	2.557E+09	9.322E+07
63.00	1.660E+09	5.243E+07	1.945E+09	6.488E+07
71.00	1.300E+09	3.745E+07	1.519E+09	4.618E+07
80.00	1.011E+09	2.684E+07	1.175E+09	3.297E+07
90.00	7.816E+08	1.905E+07	9.034E+08	2.331E+07
100.00	6.182E+08	1.363E+07	7.088E+08	1.662E+07
110.00	5.006E+08	1.200E+07	9.880E+08	5.711E+08
120.00	4.132E+08	7.598E+06	4.688E+08	9.196E+06
140.00	2.888E+08	4.841E+06	3.260E+08	5.824E+06
160.00	2.091E+08	3.741E+06	3.126E+08	2.359E+06
180.00	1.568E+08	2.109E+06	1.763E+08	2.512E+06
200.00	1.209E+08	1.484E+06	1.354E+08	1.761E+06
220.00	9.514E+07	1.087E+06	1.059E+08	1.285E+06
250.00	6.812E+07	7.141E+05	7.584E+07	8.400E+05
280.00	5.010E+07	4.876E+05	5.550E+07	5.711E+05
320.00	3.444E+07	2.951E+05	3.836E+07	3.440E+05
350.00	2.686E+07	2.448E+05	2.107E+05	2.994E+07</td

P/2 HEO Solar Proton Fluences for Trajectory and at 1.0 AU				
	Fluence at Spacecraft		Model Fluence at 1.0 AU	
	Total Mission Fluence		Total Prediction Period	
Energy (MeV)	Integral (cm^-2)	Differential (cm^-2 MeV^-1)	Integral (cm^-2)	Differential (cm^-2 MeV^-1)
0.10	2.234E+08	4.915E+08	2.227E+08	4.916E+08
0.11	2.187E+08	4.457E+08	2.180E+08	4.458E+08
0.12	2.145E+08	4.077E+08	2.138E+08	4.078E+08
0.14	2.069E+08	3.481E+08	2.063E+08	3.482E+08
0.16	2.004E+08	3.036E+08	1.998E+08	3.036E+08
0.18	1.947E+08	2.690E+08	1.940E+08	2.691E+08
0.20	1.896E+08	2.415E+08	1.889E+08	2.416E+08
0.22	1.849E+08	2.190E+08	1.843E+08	2.191E+08
0.25	1.788E+08	1.921E+08	1.782E+08	1.922E+08
0.28	1.733E+08	1.711E+08	1.728E+08	1.711E+08
0.32	1.669E+08	1.492E+08	1.664E+08	1.492E+08
0.35	1.627E+08	1.361E+08	1.621E+08	1.361E+08
0.40	1.563E+08	1.187E+08	1.557E+08	1.187E+08
0.45	1.507E+08	1.052E+08	1.502E+08	1.052E+08
0.50	1.457E+08	9.441E+07	1.452E+08	9.443E+07
0.55	1.412E+08	8.562E+07	1.407E+08	8.564E+07
0.63	1.348E+08	7.449E+07	1.343E+08	7.451E+07
0.71	1.292E+08	6.590E+07	1.287E+08	6.592E+07
0.80	1.236E+08	5.831E+07	1.231E+08	5.833E+07
0.90	1.181E+08	5.168E+07	1.176E+08	5.169E+07
1.00	1.132E+08	4.639E+07	1.127E+08	4.640E+07
1.10	1.088E+08	4.207E+07	1.083E+08	4.208E+07
1.20	1.047E+08	3.848E+07	1.043E+08	3.849E+07
1.40	9.760E+07	3.286E+07	9.719E+07	3.286E+07
1.60	9.145E+07	2.865E+07	9.106E+07	2.866E+07
1.80	8.604E+07	2.539E+07	8.567E+07	2.540E+07
2.00	8.122E+07	2.279E+07	8.086E+07	2.280E+07
2.20	7.691E+07	2.036E+07	7.655E+07	2.036E+07
2.50	7.123E+07	1.750E+07	7.089E+07	1.750E+07
2.80	6.631E+07	1.530E+07	6.598E+07	1.530E+07
3.20	6.065E+07	1.298E+07	6.035E+07	1.299E+07
3.50	5.697E+07	1.158E+07	5.667E+07	1.158E+07
4.00	5.163E+07	9.768E+06	5.135E+07	9.770E+06
4.50	4.711E+07	8.308E+06	4.685E+07	8.310E+06
5.00	4.324E+07	7.188E+06	4.299E+07	7.190E+06
5.50	3.988E+07	6.255E+06	3.963E+07	6.256E+06
6.30	3.533E+07	5.115E+06	3.511E+07	5.117E+06
7.10	3.158E+07	4.262E+06	3.138E+07	4.263E+06
8.00	2.807E+07	3.529E+06	2.789E+07	3.530E+06
9.00	2.485E+07	2.909E+06	2.468E+07	2.910E+06
10.00	2.218E+07	2.439E+06	2.202E+07	2.440E+06
11.00	1.994E+07	2.038E+06	1.979E+07	2.039E+06
12.00	1.806E+07	1.730E+06	1.791E+07	1.731E+06
14.00	1.503E+07	1.294E+06	1.492E+07	1.294E+06
16.00	1.273E+07	1.006E+06	1.263E+07	1.006E+06
18.00	1.092E+07	8.060E+05	1.083E+07	8.061E+05
20.00	9.453E+06	6.608E+05	9.372E+06	6.610E+05
22.00	8.255E+06	5.373E+05	8.180E+06	5.374E+05
25.00	6.839E+06	4.070E+05	6.777E+06	4.071E+05
28.00	5.751E+06	3.182E+05	5.696E+06	3.183E+05
32.00	4.645E+06	2.349E+05	4.602E+06	2.349E+05
35.00	4.008E+06	1.897E+05	3.969E+06	1.897E+05
40.00	3.189E+06	1.380E+05	3.159E+06	1.380E+05
45.00	2.587E+06	1.028E+05	2.563E+06	1.028E+05
50.00	2.132E+06	7.898E+04	2.112E+06	7.900E+04
55.00	1.781E+06	6.140E+04	1.764E+06	6.141E+04
63.00	1.365E+06	4.269E+04	1.353E+06	4.270E+04
71.00	1.071E+06	3.074E+04	1.063E+06	3.075E+04
80.00	8.340E+05	2.199E+04	8.287E+05	2.200E+04
90.00	6.460E+05	1.560E+04	6.432E+05	1.560E+04
100.00	5.110E+05	1.140E+04	5.096E+05	1.140E+04
110.00	4.119E+05	8.428E+03	4.115E+05	8.430E+03
120.00	3.378E+05	6.399E+03	3.379E+05	6.400E+03
140.00	2.345E+05	3.928E+03	2.373E+05	3.929E+03
160.00	1.695E+05	2.574E+03	1.735E+05	2.574E+03
180.00	1.260E+05	1.772E+03	1.307E+05	1.773E+03
200.00	9.561E+04	1.270E+03	1.006E+05	1.270E+03
220.00	7.376E+04	9.156E+02	7.900E+04	9.158E+02
250.00	5.116E+04	5.905E+02	5.686E+04	5.907E+02
280.00	3.630E+04	4.003E+02	4.224E+04	4.004E+02
320.00	2.328E+04	2.508E+02	2.951E+04	2.509E+02
350.00	1.679E+04	1.821E+02	2.308E+04	1.821E+02
400.00	9.409E+03	1.130E+02	1.588E+04	1.130E+02
450.00	4.789E+03	7.182E+01	1.136E+04	7.183E+01
500.00	1.796E+03	4.789E+01	8.414E+03	4.790E+01

Figure 18: The P/2 HEO Solar Particle Emission Spectrum.

Date	F_{10} MeV	σ_{F10}	F_{30} MeV	σ_{F30}	F_{60} MeV	σ_{F60}	F_{100} MeV	σ_{F100}	F_{200} MeV	σ_{F200}	
1984	1.0500E+09	2.5300E+07	1.8000E+08	4.8500E+06	4.3000E+07	8.1900E+05	1.3900E+07	3.0800E+05	3.4200E+06	2.4500E+05	
1985	8.3100E+07	2.7900E+06	1.2200E+07	8.8100E+05	4.2300E+06	3.4900E+05	1.8600E+06	2.6600E+05	5.9200E+05	2.5300E+05	
1986	2.6900E+08	6.7700E+06	4.8800E+07	1.1900E+06	1.3300E+07	5.7100E+05	4.5700E+06	4.0000E+05	1.1700E+06	4.0000E+05	
1987	3.0100E+07	2.1400E+06	2.3500E+06	6.8200E+05	6.9600E+05	3.5400E+05	3.5400E+05	3.1200E+05	1.5000E+05	3.2700E+05	
1988	1.4400E+08	7.7100E+06	2.7700E+07	1.7300E+06	9.9700E+06	8.1400E+05	5.1500E+06	5.1000E+05	1.9800E+06	5.0300E+05	
1989	3.2300E+10	8.5700E+08	8.8800E+09	1.6600E+08	2.7200E+09	4.2300E+06	9.3500E+08	1.5200E+06	2.1700E+08	9.2600E+05	
1990	1.1400E+09	3.2600E+07	2.1800E+08	6.6500E+06	8.0500E+07	1.0400E+06	3.6300E+07	4.1600E+05	1.1000E+07	3.4400E+05	
1991	1.1800E+10	4.7100E+08	2.9100E+09	1.5300E+08	6.0200E+08	3.6500E+06	1.2300E+08	6.7400E+05	1.8100E+07	4.6900E+05	
1992	3.9700E+09	3.7500E+08	9.6600E+08	3.7600E+07	2.3500E+08	2.1300E+06	6.4400E+07	6.4400E+05	1.3500E+07	5.6400E+05	
1993	4.1000E+07	2.8400E+06	1.0200E+07	1.2000E+06	3.2800E+06	4.2400E+05	1.3200E+06	3.3600E+05	4.0300E+05	3.3800E+05	
1994	6.7600E+08	1.1900E+08	7.2400E+06	9.5100E+05	7.2400E+06	3.7400E+05	7.2400E+06	3.3600E+05	7.2400E+06	3.4800E+05	
1995	1.9000E+07	1.5600E+06	1.5700E+06	3.2800E+05	2.7200E+05	2.4700E+05	9.2500E+04	2.0300E+05	3.1400E+04	2.1300E+05	
1996	4.8200E+05	4.8500E+05	3.9600E+04	1.9000E+05	1.6700E+04	9.0200E+04	1.2700E+04	9.2900E+04	8.0600E+03	1.0300E+05	
1997	5.1100E+08	1.1600E+07	1.7900E+08	3.4000E+06	6.8600E+07	6.2000E+06	2.8800E+07	3.4200E+05	8.0800E+06	2.9100E+05	
1998	2.2100E+09	3.0800E+07	4.3200E+08	4.0000E+06	8.6900E+07	2.0300E+06	2.0300E+07	3.8900E+05	4.4600E+06	8.2700E+05	
1999	1.2500E+08	8.4200E+06	1.3800E+07	1.1100E+06	3.9800E+06	6.0100E+05	1.8700E+06	4.5100E+05	7.3000E+05	4.5500E+05	
2000	2.2800E+10	7.9400E+07	6.8400E+09	2.5900E+07	1.7200E+09	3.2900E+06	4.1000E+08	9.5500E+05	6.2400E+07	6.4100E+05	
2001	2.6100E+10	1.0400E+08	5.3800E+09	1.1400E+07	1.1100E+09	4.0000E+06	2.4400E+08	8.6200E+05	3.8700E+07	5.9600E+05	
2002	3.3700E+09	3.8900E+08	6.8900E+08	6.1800E+06	1.4400E+08	1.6300E+06	3.0400E+07	5.8300E+05	4.3800E+06	5.4300E+05	
2003	1.3700E+10	5.7000E+08	3.5500E+09	6.1500E+07	8.2600E+08	4.6500E+06	1.8700E+08	1.0900E+06	2.5400E+07	4.3400E+05	
2004	7.2300E+08	1.6600E+07	5.7300E+07	1.4500E+06	1.1400E+07	7.8200E+05	3.5900E+06	4.1400E+05	9.2600E+05	4.1600E+05	
2005	6.1900E+09	1.2200E+08	1.4200E+09	1.7000E+07	4.1100E+08	3.2900E+06	1.4900E+08	1.6700E+06	4.2000E+07	1.2200E+06	
2006	2.4300E+09	6.2600E+08	5.4400E+08	6.1900E+06	1.5500E+08	1.4500E+06	5.1100E+07	4.5700E+05	1.1000E+07	2.5800E+05	
2007	3.4800E+04	9.5300E+04	3.3600E+04	8.8900E+04	2.9100E+04	5.0500E+04	2.1700E+04	4.9500E+04	1.3400E+04	5.4500E+04	
2008											
2009											
2010	6.3300E+06	2.1900E+06	8.5600E+05	4.8400E+05	2.6600E+05	2.4800E+05	1.9600E+05	2.4900E+05	1.1900E+05	2.6400E+05	
2011	3.8700E+08	1.6500E+07	5.8500E+07	2.3800E+06	1.8100E+07	1.0000E+06	7.5300E+04	8.6100E+05	2.4100E+06	8.7200E+05	
2012	8.6000E+09	2.8700E+08	1.5800E+09	1.2600E+07	3.5500E+08	3.6800E+06	9.3600E+07	9.7700E+05	1.5700E+07	7.7500E+05	
2013	1.1400E+09	9.1900E+07	1.1900E+08	1.9600E+06	2.5400E+07	9.2300E+05	7.6900E+06	6.3900E+05	1.8500E+06	6.2600E+05	
2014	1.4500E+09	3.3500E+07	2.0900E+08	3.8300E+06	4.4500E+07	1.1900E+06	1.2600E+07	6.2600E+05	3.1000E+06	6.0300E+05	
2015	2.3000E+08	2.2100E+07	1.2700E+07	1.3200E+06	4.7800E+06	7.3900E+05	2.7700E+06	7.1700E+05	1.3200E+06	7.4400E+05	
2016	7.6100E+06	1.5500E+06	8.6300E+05	5.0200E+05	2.1200E+05	3.0700E+05	1.4400E+05	3.0600E+05	7.8500E+04	3.2000E+05	
2017	2.1200E+09	6.8100E+07	5.9100E+08	7.4100E+06	1.8300E+08	1.5600E+06	6.0600E+07	7.4100E+05	1.2100E+07	5.5600E+05	
2018	3.1400E+04	1.8600E+05									
2019											
2008		0.00E+00									
2009		0.00E+00									
2010		0.00E+00									
2011		3.14E+04									
2012		3.48E+04									
1996		4.82E+05									
2010		6.35E+06									
2011		7.61E+06									
1995		1.90E+07									
1987		3.01E+07									
1993		4.10E+07									
1985		8.31E+07									
1994		8.31E+07									
1988		1.44E+08									
1997		3.97E+08									
1998		2.21E+09									
1999		1.25E+08									
1988		1.44E+08									
2015		2.30E+08									
1986		2.69E+08									
1987		3.01E+08									
1993		4.10E+08									
1985		8.31E+08									
1994		8.31E+08									
1988		1.44E+09									
1997		5.11E+08									
1994		6.76E+08									
2004		7.23E+08									
1984		1.05E+09									
1990		1.14E+09									
1991		1.18E+09									
1992		3.11E+09									
1993		6.19E+09									
2002		3.37E+09									
1992		3.97E+09									
2005		6.19E+09									
2012		8.60E+09									
1991		1.18E+10									
2003		1.37E+10									
2000		2.28E+10									
2001		2.61E+10									
1989		3.23E+10									

Figure 19: The Earth Trailing Orbit radiation exposure data. The values are total yearly fluence, along with error, for each energy bin. Bins start at the expressed value and continue to the next bin's value. The first bin is therefore $10 \leq x < 30$ Mev.

The following charts show comparisons of orbital radiation data. Blue regions indicate integral trapped particle fluences; orange shading indicates differential trapped particle fluences; green shading indicates comparisons. The 'Difference' columns indicate the multiplier difference between the P/2 HEO orbit and the MEO and Molniya orbits, with the P/2 being the primary orbit that the others are compared to:

$$\frac{F_{Comp} - F_{HEO}}{F_{Comp}}$$

A negative sign in these columns indicates that the P/2 HEO receives a *lower* exposure than the comparison orbit in that energy range. For example, in Figure 20, in the 0.50 MeV bin, in the first green column, the value indicates that the P/2 orbit receives 14,500 times less fluence in that energy bin than does the MEO orbit.

5.1 Trapped Particle Fluence Comparison

The trapped particle fluence comparison chart is shown in Figure 20. Cells with 'F=0' values indicate that there is no significant fluence in that energy bin. An empty cell means that the P/2 orbit has

MeV Bin	Integral Trapped Proton Fluence			Factor Difference		Differential Trapped Proton Fluence			Factor Difference	
	MEO (cm ⁻²)	Molniya (cm ⁻²)	P/2 HEO (cm ⁻²)	P/s v MEO	P/2 v Molniya	MEO (cm ⁻² MeV ⁻¹)	Molniya (cm ⁻² MeV ⁻¹)	P/2 HEO (cm ⁻² MeV ⁻¹)	P/s v MEO	P/2 v Molniya
0.10	6.6230E+14	2.7167E+14	3.9740E+11	-1.67E+03	-6.83E+02	4.0461E+15	1.1604E+15	4.8000E+12	-8.42E+02	-2.41E+02
0.15	4.8519E+14	2.1970E+14	2.0440E+11	-2.37E+03	-1.07E+03	3.0384E+15	9.1870E+14	2.9200E+12	-1.04E+03	-3.14E+02
0.20	3.5846E+14	1.7980E+14	1.0540E+11	-3.40E+03	-1.70E+03	2.1911E+15	6.9770E+14	1.5450E+12	-1.42E+03	-4.51E+02
0.30	2.0805E+14	1.3006E+14	3.7620E+10	-5.53E+03	-3.46E+03	1.1790E+15	4.1695E+14	4.5980E+11	-2.56E+03	-9.06E+02
0.40	1.2266E+14	9.6414E+13	1.3470E+10	-9.11E+03	-7.16E+03	6.7586E+14	2.7559E+14	1.6290E+11	-4.15E+03	-1.69E+03
0.50	7.2880E+13	7.4943E+13	5.0360E+09	-1.45E+04	-1.49E+04	3.9489E+14	1.8592E+14	5.7880E+10	-6.82E+03	-3.21E+03
0.60	4.3684E+13	5.9230E+13	1.8940E+09	-2.31E+04	-3.13E+04	2.2969E+14	1.3297E+14	2.1610E+10	-1.06E+04	-6.15E+03
0.70	2.6943E+13	4.8350E+13	7.1370E+08	-3.78E+04	-6.77E+04	1.4303E+14	9.8403E+13	9.4160E+09	-1.52E+04	-1.04E+04
1.00	5.9875E+12	2.8186E+13	4.0560E+07	-1.48E+05	-6.95E+05	4.7703E+13	5.2449E+13	1.4330E+09	-3.33E+04	-3.66E+04
1.50	5.9288E+11	1.4265E+13	4.8310E+05	-1.23E+06	-2.95E+07	5.9277E+12	1.9915E+13	4.0560E+07	-1.46E+05	-4.91E+05
2.00	5.9792E+10	8.2706E+12	0.0000E+00		F=0	7.2984E+11	9.2959E+12	6.4410E+05	-1.13E+06	-1.44E+07
3.00	2.6396E+09	4.3603E+12	0.0000E+00		F=0	2.9837E+10	2.8528E+12	0.0000E+00		F=0
4.00	1.1758E+08	2.5650E+12	0.0000E+00		F=0	1.3170E+09	1.3396E+12	0.0000E+00		F=0
5.00	5.6953E+06	1.6812E+12	0.0000E+00		F=0	5.8575E+07	7.1665E+11	0.0000E+00		F=0
6.00	4.3058E+05	1.1317E+12	0.0000E+00		F=0	2.8477E+06	4.4204E+11	0.0000E+00		F=0
7.00	0.0000E+00	7.9709E+11	0.0000E+00	F=0	F=0	3.2293E+05	2.9147E+11	0.0000E+00		F=0
10.00	0.0000E+00	3.1135E+11	0.0000E+00	F=0	F=0	0.0000E+00	1.1768E+11	0.0000E+00	F=0	F=0
15.00	0.0000E+00	9.1613E+10	0.0000E+00	F=0	F=0	0.0000E+00	2.7002E+10	0.0000E+00	F=0	F=0
20.00	0.0000E+00	4.1334E+10	0.0000E+00	F=0	F=0	0.0000E+00	7.5029E+09	0.0000E+00	F=0	F=0
30.00	0.0000E+00	1.7361E+10	0.0000E+00	F=0	F=0	0.0000E+00	1.4707E+09	0.0000E+00	F=0	F=0
40.00	0.0000E+00	1.1920E+10	0.0000E+00	F=0	F=0	0.0000E+00	4.4906E+08	0.0000E+00	F=0	F=0
50.00	0.0000E+00	8.3793E+09	0.0000E+00	F=0	F=0	0.0000E+00	2.6031E+08	0.0000E+00	F=0	F=0
60.00	0.0000E+00	6.7138E+09	0.0000E+00	F=0	F=0	0.0000E+00	1.3981E+08	0.0000E+00	F=0	F=0
70.00	0.0000E+00	5.5831E+09	0.0000E+00	F=0	F=0	0.0000E+00	1.0329E+08	0.0000E+00	F=0	F=0
100.00	0.0000E+00	3.3633E+09	0.0000E+00	F=0	F=0	0.0000E+00	5.9252E+07	0.0000E+00	F=0	F=0
150.00	0.0000E+00	1.6292E+09	0.0000E+00	F=0	F=0	0.0000E+00	2.5631E+07	0.0000E+00	F=0	F=0
200.00	0.0000E+00	8.0025E+08	0.0000E+00	F=0	F=0	0.0000E+00	1.2878E+07	0.0000E+00	F=0	F=0
300.00	0.0000E+00	2.5288E+08	0.0000E+00	F=0	F=0	0.0000E+00	3.5936E+06	0.0000E+00	F=0	F=0
400.00	0.0000E+00	8.1532E+07	0.0000E+00	F=0	F=0	0.0000E+00	0.0000E+00	0.0000E+00	F=0	F=0

Figure 20: Comparison of the fluence values of the P/2 HEO orbit to the MEO and Molniya orbits. A negative sign indicates that the P/2 is exposed to less trapped particle fluence by the given multiplier. A cell value of 'F=0' indicates that there is no fluence from that range of particle energies.

reached zero while the comparison orbit has not.

5.2 Solar Proton Fluence Comparison

The solar proton fluence comparison chart is shown in Figure 21. The relative scarcity of ETO data points, and the energy value mismatch at several of those points, limits the P/2 HEO comparison significantly.

6 Conclusions

The purpose of this brief paper is to compare the proton fluence results for a one-year segment of a mission on each of four orbits under consideration. Proton fluences for three of the orbits, the MEO, the Molniya and the P/s HEO, were generated by SPENVIS, using the considerations discussed in Section 4.1.2. Fluences for the ETO orbit were the results of in situ measurements taken by the NOAA GEOS-R satellites, as discussed in Section 4.5.

6.1 Trapped Particle Exposure

As noted in the previous sections, the MEO and Molniya orbits have considerable intersection with both the proton and electron regions of the Van Allen belts, while the P/2 HEO in its science orbit has no intersection. We would expect to see this reflected in the trapped particle fluences, and we do.

MeV Bin	Integral Solar Proton Fluence				Difference			Differential Solar Proton Fluence			Difference	
	MEO SPF PS (cm ⁻²)	Molniya (cm ⁻²)	P/2 HEO (cm ⁻²)	ETO High (1989) (cm ⁻²)	P/s v MEO	P/2 v Molniya	P/2 v ETO	MEO SPF PS (cm ⁻² MeV ⁻¹)	Molniya (cm ⁻² MeV ⁻¹)	P/2 HEO (cm ⁻² MeV ⁻¹)	P/s v MEO	P/2 v Molniya
0.1	8.3190E+11	9.5550E+11	2.2340E+08		-3.72E+03	-4.28E+03		5.5480E+12	6.3730E+12	4.9150E+08	-1.13E+04	-1.30E+04
0.1	7.8010E+11	8.9600E+11	2.1870E+08		-3.57E+03	-4.10E+03		4.8110E+12	5.5260E+12	4.4570E+08	-1.08E+04	-1.24E+04
0.1	7.3520E+11	8.4440E+11	2.1450E+08		-3.43E+03	-3.94E+03		4.1690E+12	4.7890E+12	4.0770E+08	-1.02E+04	-1.17E+04
0.1	6.6110E+11	7.5940E+11	2.0690E+08		-3.19E+03	-3.67E+03		3.2340E+12	3.7150E+12	3.4810E+08	-9.29E+03	-1.07E+04
0.2	6.0310E+11	6.9270E+11	2.0040E+08		-3.01E+03	-3.46E+03		2.5730E+12	2.9550E+12	3.0360E+08	-8.47E+03	-9.73E+03
0.2	5.5630E+11	6.3900E+11	1.9470E+08		-2.86E+03	-3.28E+03		2.1040E+12	2.4170E+12	2.6900E+08	-7.82E+03	-8.98E+03
0.2	5.1760E+11	5.9460E+11	1.8960E+08		-2.73E+03	-3.14E+03		1.7590E+12	2.0200E+12	2.4150E+08	-7.28E+03	-8.36E+03
0.2	4.8510E+11	5.5720E+11	1.8490E+08		-2.62E+03	-3.01E+03		1.5000E+12	1.7230E+12	2.1900E+08	-6.85E+03	-7.87E+03
0.3	4.4440E+11	5.1040E+11	1.7880E+08		-2.48E+03	-2.85E+03		1.2120E+12	1.3920E+12	1.9210E+08	-6.31E+03	-7.25E+03
0.3	4.1120E+11	4.7230E+11	1.7330E+08		-2.37E+03	-2.72E+03		1.0010E+12	1.1500E+12	1.7110E+08	-5.85E+03	-6.72E+03
0.3	3.7520E+11	4.3100E+11	1.6690E+08		-2.25E+03	-2.58E+03		7.9790E+11	9.1650E+11	1.4920E+08	-5.35E+03	-6.14E+03
0.4	3.5290E+11	4.0540E+11	1.6270E+08		-2.17E+03	-2.49E+03		6.8590E+11	7.8780E+11	1.3610E+08	-5.04E+03	-5.79E+03
0.4	3.2200E+11	3.6990E+11	1.5630E+08		-2.06E+03	-2.37E+03		5.4930E+11	6.3100E+11	1.1870E+08	-4.63E+03	-5.31E+03
0.5	2.9710E+11	3.4130E+11	1.5070E+08		-1.97E+03	-2.26E+03		4.4930E+11	5.1610E+11	1.0520E+08	-4.27E+03	-4.90E+03
0.5	2.7650E+11	3.1760E+11	1.4570E+08		-1.90E+03	-2.18E+03		3.7560E+11	4.3140E+11	9.4410E+07	-3.98E+03	-4.57E+03
0.6	2.5910E+11	2.9760E+11	1.4120E+08		-1.83E+03	-2.11E+03		3.2050E+11	3.6810E+11	8.5620E+07	-3.74E+03	-4.30E+03
0.6	2.3600E+11	2.7110E+11	1.3480E+08		-1.75E+03	-2.01E+03		2.5560E+11	2.9360E+11	7.4490E+07	-3.43E+03	-3.94E+03
0.7	2.1740E+11	2.4980E+11	1.2920E+08		-1.68E+03	-1.93E+03		2.0860E+11	2.3970E+11	6.5900E+07	-3.16E+03	-3.64E+03
0.8	2.0040E+11	2.3020E+11	1.2360E+08		-1.62E+03	-1.86E+03		1.7060E+11	1.9600E+11	5.8310E+07	-2.92E+03	-3.36E+03
0.9	1.8490E+11	2.1240E+11	1.1810E+08		-1.56E+03	-1.80E+03		1.3970E+11	1.6050E+11	5.1680E+07	-2.70E+03	-3.10E+03
1.0	1.7200E+11	1.9760E+11	1.1320E+08		-1.52E+03	-1.74E+03		1.1680E+11	1.3410E+11	4.6390E+07	-2.52E+03	-2.89E+03
1.1	1.6120E+11	1.8520E+11	1.0880E+08		-1.48E+03	-1.70E+03		9.9330E+10	1.1410E+11	4.2070E+07	-2.36E+03	-2.71E+03
1.2	1.5200E+11	1.7460E+11	1.0470E+08		-1.45E+03	-1.67E+03		8.6080E+10	9.8880E+10	3.8480E+07	-2.24E+03	-2.57E+03
1.4	1.3670E+11	1.5700E+11	9.7600E+07		-1.40E+03	-1.61E+03		6.6770E+10	7.6700E+10	3.2860E+07	-2.03E+03	-2.33E+03
1.6	1.2470E+11	1.4320E+11	9.1450E+07		-1.36E+03	-1.56E+03		5.3120E+10	6.1020E+10	2.8650E+07	-1.85E+03	-2.13E+03
1.8	1.1500E+11	1.3210E+11	8.6040E+07		-1.34E+03	-1.53E+03		4.3450E+10	4.9910E+10	2.5390E+07	-1.71E+03	-1.96E+03
2.0	1.0710E+11	1.2300E+11	8.1220E+07		-1.32E+03	-1.51E+03		3.6320E+10	4.1710E+10	2.2790E+07	-1.59E+03	-1.83E+03
2.2	1.0030E+11	1.1530E+11	7.6910E+07		-1.30E+03	-1.50E+03		3.0970E+10	3.5580E+10	2.0360E+07	-1.52E+03	-1.75E+03
2.5	9.1930E+10	1.0560E+11	7.1230E+07		-1.29E+03	-1.48E+03		2.5020E+10	2.8740E+10	1.7500E+07	-1.43E+03	-1.64E+03
2.8	8.4920E+10	9.7560E+10	6.6310E+07		-1.28E+03	-1.47E+03		2.1690E+10	2.4910E+10	1.5300E+07	-1.42E+03	-1.63E+03
3.2	7.6650E+10	8.8050E+10	6.0650E+07		-1.26E+03	-1.45E+03		1.9690E+10	2.2610E+10	1.2980E+07	-1.52E+03	-1.74E+03
3.5	7.1050E+10	8.1620E+10	5.6970E+07		-1.25E+03	-1.43E+03		1.7640E+10	2.0270E+10	1.1580E+07	-1.52E+03	-1.75E+03
4.0	6.3190E+10	7.2600E+10	5.1630E+07		-1.22E+03	-1.41E+03		1.3780E+10	1.5830E+10	9.7680E+06	-1.41E+03	-1.62E+03
4.5	5.6990E+10	6.5480E+10	4.7110E+07		-1.21E+03	-1.39E+03		1.1010E+10	1.2650E+10	8.3080E+06	-1.32E+03	-1.52E+03
5.0	5.1850E+10	5.9570E+10	4.3240E+07		-1.20E+03	-1.38E+03		9.5740E+09	1.1000E+10	7.1880E+06	-1.33E+03	-1.53E+03
5.5	4.7320E+10	5.4360E+10	3.9880E+07		-1.19E+03	-1.36E+03		8.5460E+09	9.8160E+09	6.2550E+06	-1.37E+03	-1.57E+03
6.3	4.1270E+10	4.7420E+10	3.5330E+07		-1.17E+03	-1.34E+03		6.5690E+09	7.5450E+09	5.1150E+06	-1.28E+03	-1.47E+03
7.1	3.6490E+10	4.1930E+10	3.1580E+07		-1.15E+03	-1.33E+03		5.3810E+09	6.1800E+09	4.6260E+06	-1.26E+03	-1.45E+03
8.0	3.2080E+10	3.6860E+10	2.8070E+07		-1.14E+03	-1.31E+03		4.4210E+09	5.0780E+09	3.5290E+06	-1.25E+03	-1.44E+03
9.0	2.8150E+10	3.2350E+10	2.4850E+07		-1.13E+03	-1.30E+03		3.4410E+09	3.9530E+09	2.9090E+06	-1.18E+03	-1.36E+03
10.0	2.4980E+10	2.8710E+10	2.2180E+07	3.2300E+10	-1.12E+03	-1.29E+03	-1.46E+03	2.8900E+09	3.3190E+09	2.4390E+06	-1.18E+03	-1.36E+03
11.0	2.2290E+10	2.5620E+10	1.9940E+07		-1.12E+03	-1.28E+03		2.4880E+09	2.8580E+09	2.0380E+06	-1.22E+03	-1.40E+03
12.0	2.0020E+10	2.3010E+10	1.8060E+07		-1.11E+03	-1.27E+03		2.0570E+09	2.3630E+09	1.7300E+06	-1.19E+03	-1.36E+03
14.0	1.6470E+10	1.8930E+10	1.5030E+07		-1.09E+03	-1.26E+03		1.4980E+09	1.7210E+09	1.2940E+06	-1.16E+03	-1.33E+03
16.0	1.3810E+10	1.5880E+10	1.2730E+07		-1.08E+03	-1.25E+03		1.1540E+09	1.3250E+09	1.0060E+06	-1.15E+03	-1.32E+03
18.0	1.1770E+10	1.3530E+10	1.0920E+07		-1.08E+03	-1.24E+03		8.9590E+08	1.0290E+09	8.0600E+05	-1.11E+03	-1.28E+03
20.0	1.0150E+10	1.1680E+10	9.4530E+06		-1.07E+03	-1.23E+03		7.1610E+08	8.2250E+08	6.6080E+05	-1.08E+03	-1.24E+03
22.0	8.8460E+09	1.0180E+10	8.2550E+06		-1.07E+03	-1.23E+03		5.9140E+08	6.7930E+08	5.3730E+05	-1.10E+03	-1.26E+03
25.0	7.2950E+09	8.3950E+09	6.8390E+06		-1.07E+03	-1.23E+03		4.4260E+08	5.0840E+08	4.0700E+05	-1.09E+03	-1.25E+03
28.0	6.1110E+09	7.0350E+09	5.7510E+06		-1.06E+03	-1.22E+03		3.1620E+08	3.9770E+08	3.1820E+05	-9.93E+02	-1.25E+03
30.0				8.8800E+09								
32.0	4.9190E+09	5.6660E+09	4.6450E+06		-1.06E+03	-1.22E+03		2.4990E+08	2.8710E+08	2.3490E+05	-1.06E+03	-1.22E+03
35.0	4.2420E+09	4.8880E+09	4.0080E+06		-1.06E+03	-1.22E+03		2.0140E+08	2.3140E+08	1.8970E+05	-1.06E+03	-1.22E+03
40.0	3.3710E+09	3.8870E+09	3.1890E+06		-1.06E+03	-1.22E+03		1.4700E+08	1.6920E+08	1.3800E+05	-1.06E+03	-1.23E+03
45.0	2.7310E+09	3.1500E+09	2.5870E+06		-1.05E+03	-1.22E+03		1.0900E+08	1.2570E+08	1.0280E+05	-1.06E+03	-1.22E+03
50.0	2.2520E+09	2.5960E+09	2.1320E+06		-1.06E+03	-1.22E+03		8.2750E+07	9.5570E+07	7.8980E+04	-1.05E+03	-1.21E+03
55.0	1.8830E+09	2.1700E+09	1.7810E+06		-1.06E+03	-1.22E+03		6.4850E+07	7.5060E+07	6.1400E+04	-1.06E+03	-1.22E+03
60.0				2.7200E+09								
63.0	1.4420E+09	1.6600E+09	1.3650E+06		-1.06E+03	-1.22E+03		4.5140E+07	5.2430E+07	4.2690E+04	-1.06E+03	-1.23E+03
71.0	1.1340E+09	1.3000E+09	1.0710E+06		-1.06E+03	-1.21E+03		3.2130E+07	3.7450E+07	3.0740E+04	-1.04E+03	-1.22E+03
80.0	8.8630E+08	1.0110E+09	8.3400E+05		-1.06E+03	-1.21E+03		2.2940E+07	2.6840E+07	2.1990E+04	-1.04E+03	-1.22E+03
90.0	6.9050E+08	7.8160E+08	6.4600E+05		-1.07E+03	-1.21E+03		1.6220E+07	1.9050E+07	1.5600E+04	-1.04E+03	-1.22E+03
100.0	5.5150E+08	6.1820E+08	5.1100E+05	9.3500E+08	-1.08E+03	-1.21E+03	-1.83E+03	1.1580E+07	1.3630E+07	1.1400E+04	-1.01E+03	-1.19E+03
110.0	4.5160E+08	5.0060E+08	4.1190E+05		-1.10E+03	-1.21E+03		8.4040E+06	9.8800E+06	8.4280E+03	-9.96E+02	-1.17E+03
120.0	3.7710E+08	4.1290E+08	3.3780E+05		-1.12E+03	-1.22E+03		6.4910E+06	7.5980E+06	6.3990E+03	-1.01E+03	-1.19E+03
140.0	2.7020E+08	2.8880E+08	2.3450E+05		-1.15E+03</td							

The MEO (and EMEO) orbit intersects the outer region of the proton belts, and so is exposed to mostly lower energy protons. This is reflected in its proton spectra by its proton fluence dropping to zero at around 7.0 MeV. However, a glance at the intersection image shows that both the MEO and the EMEO orbits intersect the region of the *highest* energy electron belts. The loss of high energy proton fluence is countered by the gain in high energy electron fluence.

Whereas the MEO and EMEO orbits are constantly immersed in the belts, the Molniya's intersection occurs for a small portion of its orbit, on the approach and departure from perigee, but it is still enough to crank its fluence levels to fairly high levels. During the time it passes through its two mirror image exposures, it manages to pass through all energy level zones of both protons and electrons, and this is reflected by having relatively high fluence values across its entire spectrum.

Given that the P/2 avoids the belts entirely during its science trajectory, its only exposures to belt particles is during the initial phasing orbits (which is not included in these calculations), and in the science orbit when it is exposed to the cloud of low energy particles that get distributed outwards from the belt as a result of the solar wind. (This affects the Molniya orbit as well.)

Conclusion: *The P/2 orbit receives significantly lower high energy trapped proton and electron fluence, by as much as seven orders of magnitude, across all energy bins, than does the MEO, EMEO, or Molniya orbits.*

6.2 Solar Proton Exposure

Similarly, in terms of high energy solar proton fluence, the P/2 also receives significantly less fluence across all energy bins than does the MEO or Molniya orbit. And, perhaps not surprisingly, given the ETO orbit's position outside of the magnetosphere, the P/2 also receives less fluence than does the ETO orbit, although admittedly comparison data points for the ETO are limited.

Conclusion: *The P/2 orbit receives significantly lower high energy solar proton fluence, by three orders of magnitude, across all energy bins, than does the MEO, EMEO, or Molniya orbits.*

6.3 Summary

None of this is actually surprising, given several factors. The P/2 orbit is a masterpiece of orbital design, and was specifically engineered to avoid the Van Allen belts, reducing its exposure to trapped particle fluence. But it remains comfortably inside the magnetosphere, reducing its exposure to solar protons.

Given the other considerations the designers took into consideration, such as the precise counteracting of solar and lunar perturbances to create a highly stable orbit and the reduction of orbital eclipsing, the low radiation profile of the P/2 orbit is yet another reason to recommend the P/2 Highly Elliptical Orbit.

Appendices

A Table of Solar Proton Events

A problem with adopting an Earth Trailing Orbit is that missions under consideration utilize off-the shelf components for mission-critical instruments. These components are not radiation hardened. The ETO orbit is constantly exposed to solar proton events, and is therefore at the mercy of constant bombardment by high energy solar protons and the unpredictability of major solar events.

I have included tables reprinted from Raukunen and Usoskin's 2022 article *Annual integral solar proton fluences for 1984-2019* as a reminder of the extreme variability in solar proton events. A glance through Figures 22 and 23 show the extreme output that these solar discharges produce.

Particle Events

Year	Start (Day/UT)	Maximum (Day/UT)	Proton Flux (pfu@>10 MeV)		Year	Start (Day/UT)	Maximum (Day/UT)	Proton Flux (pfu@>10 MeV)
1976	Apr 30/2120	May 01/1700	12		1988	Jan 02/2325	Jan 03/0835	92
1977	Sep 19/1430	Sep 19/2130	200		1988	Mar 25/2225	Mar 25/2330	58
1977	Nov 22/1400	Nov 22/1800	160		1988	Jun 30/1055	Jun 30/1140	21
					1988	Aug 26/0000	Aug 26/0045	42
1978	Feb 13/0930	Feb 14/1000	850		1988	Oct 12/0920	Oct 12/0930	12
1978	Apr 11/1530	Apr 11/1630	65		1988	Nov 08/2225	Nov 09/0635	13
1978	Apr 29/0445	Apr 30/2000	1000		1988	Nov 14/0130	Nov 14/0235	13
1978	May 07/0420	May 07/0420	100		1988	Dec 17/0610	Dec 17/0855	18
1978	Jun 02/0730	Jun 02/0935	19		1988	Dec 17/2000	Dec 18/0150	29
1978	Jun 24/0900	Jun 25/0230	25					
1978	Jul 13/0300	Jul 13/1000	20		1989	Jan 04/2305	Jan 05/0130	28
1978	Sep 23/1035	Sep 24/0400	2200		1989	Mar 08/1735	Mar 13/0645	3500
1978	Nov 10/2130	Nov 10/2140	38		1989	Mar 17/1855	Mar 18/0920	2000
					1989	Mar 23/2040	Mar 24/0110	53
1979	Feb 17/2020	Feb 17/2205	31		1989	Apr 11/1435	Apr 12/0125	450
1979	Apr 03/1600	Apr 03/2310	45		1989	May 05/0905	May 05/1000	27
1979	Jun 06/1850	Jun 07/0005	950		1989	May 06/0235	May 06/1045	110
1979	Jul 07/0015	Jul 07/1010	50		1989	May 23/1135	May 23/1350	68
1979	Aug 19/0850	Aug 21/0740	500		1989	May 24/0730	May 24/0905	15
1979	Sep 15/1500	Sep 16/1200	60		1989	Jun 18/1650	Jun 18/1910	18
1979	Nov 16/0430	Nov 16/1300	75		1989	Jun 30/0655	Jun 30/0710	17
					1989	Jul 01/0655	Jul 01/0720	17
1980	Feb 06/1340	Feb 06/1850	12		1989	Jul 25/0900	Jul 25/1225	54
1980	Jul 17/2300	Jul 19/1930	100		1989	Aug 12/1600	Aug 13/0710	9200
					1989	Sep 04/0120	Sep 04/0510	44
1981	Mar 30/0900	Mar 30/2115	30		1989	Sep 12/1935	Sep 13/0825	57
1981	Apr 10/1745	Apr 11/1400	50		1989	Sep 29/1205	Sep 30/0210	4500
1981	Apr 24/1515	Apr 24/2330	160		1989	Oct 06/0050	Oct 06/0825	22
1981	May 09/1200	May 10/2130	150		1989	Oct 19/1305	Oct 20/1600	40000
1981	May 15/0300	May 16/1950	130		1989	Nov 09/0240	Nov 09/0610	43
1981	Jul 20/1430	Jul 20/1825	100		1989	Nov 15/0735	Nov 15/0910	71
1981	Jul 25/0600	Jul 25/1320	18		1989	Nov 27/2000	Nov 28/1105	380
1981	Aug 10/0115	Aug 10/0435	57		1989	Nov 30/1345	Dec 01/1340	7300
1981	Oct 08/1235	Oct 13/2247	2000					
1981	Dec 10/0545	Dec 11/0900	65		1990	Mar 19/0705	Mar 19/2315	950
					1990	Mar 29/0915	Mar 29/1005	16
1982	Jan 31/0055	Jan 31/1630	830		1990	Apr 07/2240	Apr 08/1330	18
1982	Jun 06/0245	Jun 06/0245	10		1990	Apr 11/2120	Apr 11/2130	13
1982	Jun 09/0040	Jun 09/0510	30		1990	Apr 17/0500	Apr 17/0655	12
1982	Jul 11/0700	Jul 13/1615	2900		1990	Apr 28/1005	Apr 28/1735	150
1982	Jul 22/2030	Jul 23/0220	240		1990	May 21/2355	May 22/0750	410
1982	Sep 05/2205	Sep 06/0100	66		1990	May 24/2125	May 25/0115	180
1982	Nov 22/1940	Nov 22/2140	40		1990	May 28/0715	May 29/0100	45
1982	Nov 26/0605	Nov 26/1500	25		1990	Jun 12/1140	Jun 12/1700	79
1982	Dec 08/0010	Dec 08/1000	1000		1990	Jul 26/1720	Jul 26/2315	21
1982	Dec 17/1845	Dec 18/0945	130		1990	Aug 01/0000	Aug 01/2015	230
1982	Dec 19/1920	Dec 20/0515	85					
					1991	Jan 31/1130	Jan 31/1620	240
1982	Dec 27/0600	Dec 27/1345	190		1991	Feb 25/1210	Feb 25/1305	13
					1991	Mar 23/0820	Mar 24/0350	43000
1983	Feb 03/1200	Feb 04/1620	340		1991	Mar 29/2120	Mar 30/0330	20
1983	Jun 15/0435	Jun 15/1800	18		1991	Apr 03/0815	Apr 04/1000	52
					1991	May 13/0300	May 13/0910	350
1984	Feb 16/0915	Feb 16/1005	660		1991	May 31/1225	Jun 01/0445	22
1984	Feb 19/1310	Feb 21/1415	55		1991	Jun 04/0820	Jun 11/1420	3000
1984	Mar 13/1440	Mar 13/1450	10		1991	Jun 14/2340	Jun 15/1950	1400
1984	Mar 14/0405	Mar 14/0505	100		1991	Jun 30/0755	Jul 02/1010	110
1984	Apr 25/1330	Apr 26/1420	2500		1991	Jul 07/0455	Jul 08/1645	2300
1984	May 24/1045	May 24/1140	31		1991	Jul 11/0240	Jul 11/0450	30
1984	May 31/1315	May 31/1415	15		1991	Jul 11/2255	Jul 12/0205	14
					1991	Aug 26/1740	Aug 27/1830	240
1985	Jan 22/0415	Jan 22/0550	14		1991	Oct 01/1740	Oct 01/1810	12
1985	Apr 25/1430	Apr 26/0600	160		1991	Oct 28/1300	Oct 28/1440	40
1985	Jul 09/0235	Jul 09/0325	140		1991	Oct 30/0745	Oct 30/0810	94
1986	Feb 06/0925	Feb 07/1730	130		1992	Feb 07/0645	Feb 07/1115	78
1986	Feb 14/1155	Feb 15/0400	130		1992	Mar 16/0840	Mar 16/0840	10
1986	Mar 06/1835	Mar 06/1930	21		1992	May 09/1005	May 09/2100	4600
1986	May 04/1255	May 04/1320	16		1992	Jun 25/2045	Jun 26/0610	390
1987	Nov 08/0200	Nov 08/0940	120		1992	Aug 06/1145	Aug 06/1210	14
					1992	Oct 30/1920	Oct 31/0710	2700

Figure 22: Table of Solar Flare Proton Events, 1976-1992.

Particle Events			
Year	Start (Day/UT)	Maximum (Day/UT)	Proton Flux (pfu@>10 MeV)
1993	Mar 04/1505	Mar 04/1735	17
1993	Mar 12/2010	Mar 13/0155	44
1994	Feb 20/0300	Feb 21/0900	10000
1994	Oct 20/0030	Oct 20/0340	35
1995	Oct 20/0825	Oct 20/1210	63
1997	Nov 04/0830	Nov 04/1120	72
1997	Nov 06/1305	Nov 07/0255	490
1998	Apr 20/1400	Apr 21/1205	1700
1998	May 02/1420	May 02/1650	150
1998	May 06/0845	May 06/0945	210
1998	Aug 24/2355	Aug 26/1055	670
1998	Sep 25/0010	Sep 25/0130	44
1998	Sep 30/1525	Oct 01/0025	1200
1998	Nov 08/0245	Nov 08/0300	11
1998	Nov 14/0810	Nov 14/1240	310
1999	Jan 23/1105	Jan 23/1135	14
1999	Apr 24/1804	Apr 25/0055	32
1999	May 05/1820	May 05/1955	14
1999	Jun 02/0245	Jun 02/1010	48
1999	Jun 04/0925	Jun 04/1055	64
2000	Feb 18/1130	Feb 18/1215	13
2000	Apr 04/2055	Apr 05/0930	55
2000	Jun 07/1335	Jun 08/0940	84
2000	Jun 10/1805	Jun 10/2045	46
2000	Jul 14/1045	Jul 15/1230	24000
2000	Jul 22/1320	Jul 22/1405	17
2000	Jul 28/1050	Jul 28/1130	18
2000	Aug 11/1650	Aug 11/1655	17
2000	Sep 12/1555	Sep 13/0340	320
2000	Oct 16/1125	Oct 16/1840	15
2000	Oct 26/0040	Oct 26/0340	15
2000	Nov 08/2350	Nov 09/1600	14800
2000	Nov 24/1520	Nov 26/2030	942
2001	Jan 28/2025	Jan 29/0655	49
2001	Mar 29/1635	Mar 30/0610	35
2001	Apr 02/2340	Apr 03/0745	1110
2001	Apr 10/0850	Apr 11/2055	355
2001	Apr 15/1410	Apr 15/1920	951
2001	Apr 18/0315	Apr 18/1045	321
2001	Apr 28/0430	Apr 28/0500	57
2001	May 07/1915	May 08/0755	30
2001	Jun 15/175	Jun 16/0005	26
2001	Aug 10/1020	Aug 10/1155	17
2001	Aug 16/0135	Aug 16/0355	493
2001	Sep 15/1435	Sep 15/1455	11
2001	Sep 24/1215	Sep 25/2235	12900
2001	Oct 01/1145	Oct 02/0810	2360
2001	Oct 19/2225	Oct 19/2235	11
2001	Oct 22/1910	Oct 22/2130	24
2001	Nov 04/1705	Nov 06/0215	31700
2001	Nov 19/1230	Nov 20/0010	34
2001	Nov 22/2320	Nov 24/0555	18900
2001	Dec 26/0605	Dec 26/1115	779
2001	Dec 29/0510	Dec 29/0815	76
2001	Dec 30/0245	Dec 31/1620	108
2002	Jan 10/2045	Jan 11/0530	91
2002	Jan 15/1435	Jan 15/2000	15
2002	Feb 20/0730	Feb 20/0755	13
2002	Mar 17/0820	Mar 17/0850	13
2002	Mar 18/1300	Mar 19/0650	53
2002	Mar 20/1510	Mar 20/1525	19
2002	Mar 22/2020	Mar 23/1320	16
2002	Apr 17/1530	Apr 17/1540	24
2002	Apr 21/0225	Apr 21/2320	2520
2002	May 22/1755	May 23/1055	820
2002	Jul 07/1830	Jul 07/1955	22
2002	Jul 16/1750	Jul 17/1600	234
2002	Jul 19/1050	Jul 19/1515	13
2002	Jul 22/0655	Jul 23/1025	28
2002	Aug 14/0900	Aug 14/1620	26
2002	Aug 22/0440	Aug 22/0940	36
2002	Aug 24/0140	Aug 24/0835	317
2002	Sep 07/0440	Sep 07/1650	208
2002	Nov 09/1920	Nov 10/0540	404
Year	Start (Day/UT)	Maximum (Day/UT)	Proton Flux (pfu@>10 MeV)
2003	May 28/2335	May 29/1530	121
2003	May 31/0440	May 31/0645	27
2003	Jun 18/2050	Jun 19/0450	24
2003	Oct 26/1825	Oct 26/2235	466
2003	Oct 28/1215	Oct 29/0615	29500
2003	Nov 02/1105	Nov 03/0815	1570
2003	Nov 04/2225	Nov 05/0600	353
2003	Nov 21/2355	Nov 22/0230	13
2003	Dec 02/1505	Dec 02/1730	86
2004	Apr 11/1135	Apr 11/1845	35
2004	Jul 25/1855	Jul 26/2250	2086
2004	Sep 13/2105	Sep 14/0005	273
2004	Nov 01/0655	Nov 01/0805	63
2004	Nov 07/1910	Nov 08/0115	495
2005	Jan 16/0210	Jan 17/1750	5040
2005	May 14/0525	May 15/0240	3140
2005	Jun 16/2200	Jun 17/0500	44
2005	Jul 14/0245	Jul 15/0345	134
2005	Jul 27/2300	Jul 29/1715	41
2005	Aug 22/2040	Aug 23/1045	330
2005	Sep 08/0215	Sep 11/0425	1880
2006	Dec 06/1555	Dec 07/1930	1980
2006	Dec 13/0310	Dec 13/0925	698
2010	Aug 14/1230	Aug 14/1245	14
2011	Mar 08/0105	Mar 08/0800	50
2011	Mar 21/1950	Mar 22/0135	14
2011	Jun 07/0820	Jun 07/1820	72
2011	Aug 04/0635	Aug 05/2150	96
2011	Aug 09/0845	Aug 09/1210	26
2011	Sep 23/2255	Sep 26/1155	35
2011	Nov 26/1125	Nov 27/0125	80
2012	Jan 23/0530	Jan 24/1530	6310
2012	Jan 27/1905	Jan 28/0205	796
2012	Mar 07/0510	Mar 08/1115	6530
2012	Mar 13/1810	Mar 13/2045	469
2012	May 17/0210	May 17/0430	255
2012	May 27/0535	May 27/1045	14
2012	Jun 16/1955	Jun 16/2020	14
2012	Jul 07/0400	Jul 07/0745	25
2012	Jul 12/1835	Jul 12/2225	96
2012	Jul 17/1715	Jul 18/0600	136
2012	Jul 23/1545	Jul 23/2145	12
2012	Sep 01/1335	Sep 02/0850	59
2012	Sep 28/0300	Sep 28/0445	28
2013	Mar 16/1940	Mar 17/0700	16
2013	Apr 11/1055	Apr 11/1645	114
2013	May 15/1325	May 17/1720	41
2013	May 22/1420	May 23/0650	1660
2013	Jun 23/2014	Jun 24/0520	14
2013	Sep 30/0505	Sep 30/2005	182
2013	Dec 28/2150	Dec 28/2315	29
2014	Jan 06/0915	Jan 06/1600	42
2014	Jan 06/0915	Jan 09/0340	1033
2014	Feb 20/0850	Feb 20/0925	22
2014	Feb 25/1355	Feb 28/0845	103
2014	Apr 18/1525	Apr 19/0105	58
2014	Sep 11/0240	Sep 12/1555	126
2015	Jun 18/1135	Jun 18/1445	16
2015	Jun 21/2135	Jun 22/1900	1070
2015	Jun 26/0350	Jun 27/0030	22
2015	Oct 29/0550	Oct 29/1000	23
2016	Jan 02/0430	Jan 02/0450	21
2017	Jul 14/0900	Jul 14/2320	22
2017	Sep 05/0040	Sep 08/0035	844

Figure 23: Table of Solar Flare Proton Events, 1993-2017.

References

Note: All illustrations and tables created by author.

- [1] Eric Joffre et al. "Astrodynamics techniques for missions towards Earth trailing or leading heliocentric orbits". In: *7th International Conference on Astrodynamics Tools and Techniques (ICATT), DLR Oberpfaffenhofen, Germany*. 2018.
- [2] BT Kress et al. "Observations from NOAA's newest solar proton sensor". In: *Space Weather* 19.12 (2021), e2021SW002750.
- [3] Daniel A McGiffin, Michael Mathews, and Steven Cooley. "High Earth Orbit Design for Lunar-Assisted Medium Class Explorer Missions". In: *2001 Flight Mechanics Symposium*. 2001.
- [4] O. Raukunen et al. "Annual integral solar proton fluences for 1984-2019". In: *aap* 665 (2022).
- [5] ESA SPENVIS. 2018. URL: <https://www.spenvis.oma.be/help/background/flare/flare.html#ESP>.
- [6] ESA SPENVIS. *The Earth's trapped particle radiation environment*. 2018. URL: <https://www.spenvis.oma.be/help/background/traprad/traprad.html#APAE>.